Modern Journal of Statistics
2(1), 112–137
DOI: https://doi.org/10.64389/mjs.2026.02139
https://sphinxsp.org/journal/index.php/mjs

Research article

A New Modified Arctan Model: Statistical Properties, Estimation Methods, Simulation Study, and Real-Life Application

Ahmed M. Gemeay[1], Nooruldeen Ayad Noori [2], Khder Alakkari [3], Mundher A. Khaleel[4], Faisal A. M. Ali[5], Gizachew Tirite Gellow[6], Alexis Habineza[7], Ali T. Hammad[1, *]

[1]Department of Mathematics, Faculty of Science, Tanta University, Tanta 31527, Egypt; ahmed.gemeay@science.tanta.edu.eg

[2]Anbar Education Directorate, Anbar 31002, Iraq; Nooruldeen.a.noori35508@st.tu.edu.iq

[3]Department of Statistics and Programming, Faculty of Economics, Latakia University, Latakia, P.O. Box 2230, Syria; khderalakkari1990@gmail.com

[4]Mathematics Departments, College of Computer Science and Mathematics, Tikrit University, Tikrit 3400, Iraq; mun880088@tu.edu.iq

[5]Department of Data Science and Information Technology, Taiz University, Taiz 6803, Yemen; faisalali@taiz.edu.ye

[6]Department of Mathematics, College of Natural Science, Debre Tabor University, Debre Tabor 272, Ethiopia; drgizachew322@gmail.com

[7]Department of Mathematics, College of Science and Technology, School of Science, University of Rwanda, Kigali City, 3900, Rwanda; alexhabineza@kp.ac.rw

***Correspondence:** ali.taha@science.tanat.edu.eg

ARTICLE INFO

Keywords:
Half-Cauchy,
Arctan function,
Goodness-of-fit tests,
Diesel engines.

Mathematics Subject Classification:
37J39, 62G08

Important Dates:
Received: 5 October 2025
Revised: 24 November 2025
Accepted: 30 November 2025
Online: 1 December 2025

ABSTRACT

This study introduces the modified Weibull Arctan (MWArctan) distribution, a new model derived from the Modified Weibull-G (MWG) family using the Arctan function as a generator. The theoretical formulation of the distribution is presented through derivations of its probability density function, cumulative distribution function, survival function, and hazard function. Analytical expansions are developed to simplify the computation of statistical properties, moments, and the quantile function. Three parameter estimation methods were evaluated through a Monte Carlo simulation across various sample sizes. The MLE method consistently produced the most efficient and stable estimates, exhibiting the lowest bias, MSE, and RMSE values. In contrast, LSE demonstrated lower bias only for small samples, but higher variance. The practical applicability of the MWArctan model was verified using real-life data from 40 turbochargers in diesel engines. The proposed model achieved the best fit compared to six competing Arctan-based distributions, as indicated by specific information criteria and goodness-of-fit tests. Graphical comparisons confirmed its superior flexibility in capturing both the central tendency and tail behavior of the empirical data. These results establish MWArctan as a robust and adaptable model for analyzing reliability and lifetime data.

1. Introduction

Probability distributions play a fundamental role in applied and theoretical statistics, helping to represent data and understand the behavior of random phenomena. A large group of statistical distribution families has emerged, such as (Inverted Topp–Leone-H family [1], Shifted Exponential-G (SHE-G) generator [2], Novel Logarithmic Approach [3], NGLog-X Family [4], Lomax extended exponentiated-X [5], Odd Lomax-G family [6], Generalized Odd Maxwell-Generated [7], hybrid odd exponential [8], Modified type-II family [9]). Among the important statistical families is the Modified Weibull-G (MWG) family [10], [11], which has proven its flexibility in representing a wide variety of data types. It has the following CDF and PDF functions, respectively:

$$G(x) = 1 - e^{-\delta\left(\frac{(F(x))^2}{1-F(x)}\right)^{\beta}}, x \geq 0, \delta, \beta > 0, \tag{1}$$

$$g(x) = \delta\beta e^{-\delta\left(\frac{(F(x))^2}{1-F(x)}\right)^{\beta}} \left(\frac{(F(x))^2}{1-F(x)}\right)^{\beta-1} \frac{F(x)f(x)(2-F(x))}{(1-F(x))^2}, x \geq 0, \delta, \beta > 0, \tag{2}$$

where δ, β are shape and scale parameters for MWG respectively, and $F(x), f(x)$ are CDF and pdf for any baseline distribution respectively and x is any random variable.

The Cauchy distribution is a continuous distribution and has the following CDF and pdf functions, respectively:

$$F(x) = \frac{2}{\pi}\arctan\left(\frac{x}{\gamma}\right), x \in \mathbb{R}, \gamma > 0, \tag{3}$$

$$f(x) = \frac{2}{\pi\gamma\left(1+\left(\frac{x}{\gamma}\right)^2\right)}, x \in \mathbb{R}, \gamma > 0. \tag{4}$$

The Arctan distribution is directly related to the standard half-Cauchy distribution $(0, \infty)$ with scale parameter ($\gamma = 1$). The half-Cauchy distribution is a continuous distribution derived from Cauchy, but it is restricted to positive values. It has a scale parameter that controls the width of the distribution. It does not have a defined mean or variance and is a dense-tailed model. It is often used as a priority for scale parameters in Bayesian theory. These properties make the Arctan basis suitable for representing positive data with heavy tails. It has CDF and pdf functions, respectively, as follows:

$$F(x) = \frac{2}{\pi}\arctan(x), x \geq 0, \tag{5}$$

$$f(x) = \frac{2}{\pi(1+x^2)}, x \geq 0. \tag{6}$$

The importance of the proposed distribution lies in its high flexibility in representing heavy-tailed data or data that require more precise characterization than classical distributions such as half-Cauchy or Cauchy. Furthermore, the proposal was supported by a Monte Carlo simulation study and real data to evaluate the efficiency of the new model compared to other well-known distributions.

The research aims to establish an explicit definition of the MWArctan distribution within the MWG framework and derive the basic functions required for analysis and fitting, while illustrating their behavior graphically. It also aims to evaluate the efficiency of the three estimation methods (MLE, LSE, and WLSE) through a regularized Monte Carlo simulation, measure performance using statistical metrics, and then apply the distribution to failure time data from 40 turbochargers.

2. Modified Weibull Arctan (MWArctan) distribution

The CDF function of MWArctan distribution can be founded by combining Equation (5) with Equation (1) to get a form:

$$\boldsymbol{G(x) = 1 - e^{-\delta\left(\frac{\left(\frac{2}{\pi}arctan(x)\right)^2}{1-\frac{2}{\pi}arctan(x)}\right)^{\beta}}}, \tag{7}$$

while the pdf function of MWArctan distribution can be founded by derivative Equation (7) to get a form:

$$g(x) = 4\delta\beta e^{-\delta\left(\frac{\left(\frac{2}{\pi}arctan(x)\right)^2}{1-\frac{2}{\pi}arctan(x)}\right)^{\beta}} \left(\frac{\left(\frac{2}{\pi}arctan(x)\right)^2}{1-\frac{2}{\pi}arctan(x)}\right)^{\beta-1} \frac{arctan(x)\left(2-\frac{2}{\pi}arctan(x)\right)}{\pi^2\left(1-\frac{2}{\pi}arctan(x)\right)^2(1+x^2)}. \quad (8)$$

Figures 1 and 2 illustrate the behavior of the CDF and pdf functions for different levels of parameters.

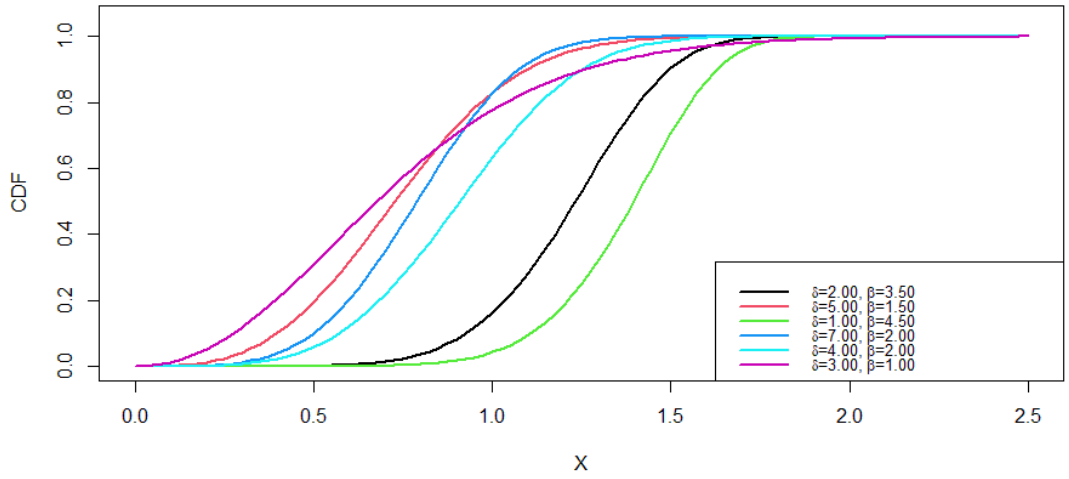

Figure 1. Plot CDF function for MWArctan distribution with different values of parameters

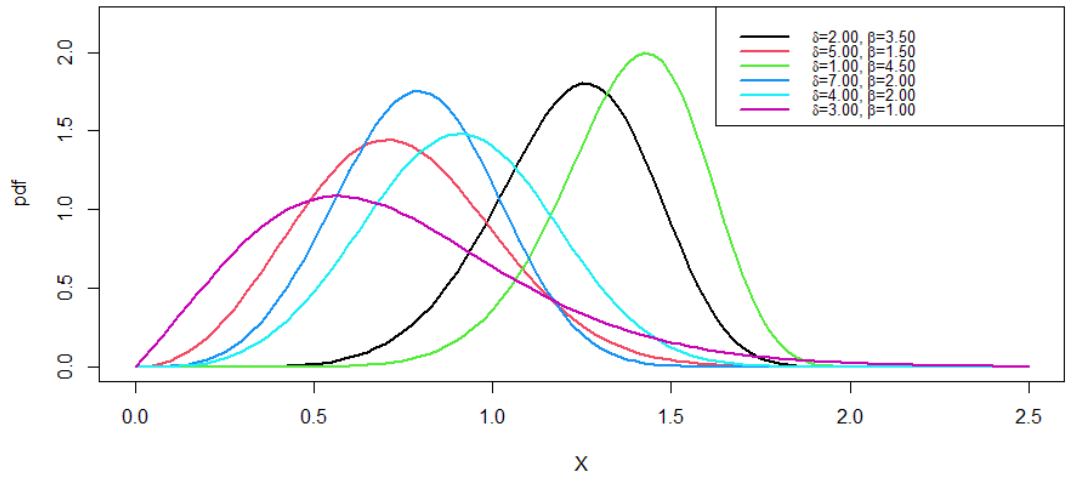

Figure 2. Plot pdf function for MWArctan distribution with different values of parameters

Figure 1 shows that curves with large δ accelerate early and reach 0.5 at smaller x values, implying faster probability accumulation in the left-hand part of the domain. The cases $\delta = 5.00, \beta = 1.50, \delta = 7.00$, and $\beta = 2.00$ cross the center quickly and then stabilize near unity before $x \approx 1.5$. In contrast, the curves with large β and small δ lag horizontally and then rise sharply around the center. The cases with $\delta = 1.00$ and $\beta = 4.50$ reach 0.5 at relatively large x and then continue the climb smoothly. The cases with $\delta = 3.00$ and $\beta = 1.00$ show an early but gradual rise, reflecting a wider spread of mass. Differences in the slope of the CDF around the center reveal differences in dispersion. A steeper slope means less dispersion, and a lower slope means more dispersion.

Figure 2 shows the sensitivity of the peak location and breadth of the distribution to changes in δ and β. As β increases with relatively small δ, a more concentrated curve appears with a higher peak at slightly larger x values. The case of $\delta = 1.00$ and $\beta = 4.50$ gives a high peak with a location close to 1.4 with less dispersion around the peak. The case of $\delta = 2.00$ and $\beta = 3.50$ remains high-peaked but less steep and with a peak closer to 1.3. As δ increases and β decreases, the curve shifts to the left and becomes broader and lower-peaked. The cases of $\delta = 5.00$ and $\beta = 1.50$ and $\delta = 7.00$ and $\beta = 2.00$ show early peaks near $0.7 - 1.0$ with faster-falling tails after the peak. With $\beta = 1.00$ and $\delta = 3.00$, the peak

becomes relatively flat, and the right tail lengthens slightly. The general reading is that increasing δ pushes the mass to the left and accelerates the early density rise, while increasing β pushes the mass to the right, raising the peak and intensifying concentration around it. The variation in peak height and amplitude across the six pairs demonstrates the remarkable shape flexibility of the distribution and its ability to represent data with early or late peaks and varying tails.

3. Some Properties for MWArctan distribution

3.1 Survival Analysis of MWArctan distribution

The survival function $S(x)$ expresses the probability of an individual surviving until time x or later, and is known as [12], [13], [14]:

$$S(x) = P(X > x) = 1 - F(x)$$

$$S(x) = e^{-\delta\left(\frac{\left(\frac{2}{\pi}arctan(x)\right)^2}{1-\frac{2}{\pi}arctan(x)}\right)^{\beta}}. \tag{9}$$

Figures 3 illustrate the behavior of the survival function for different levels of parameters.

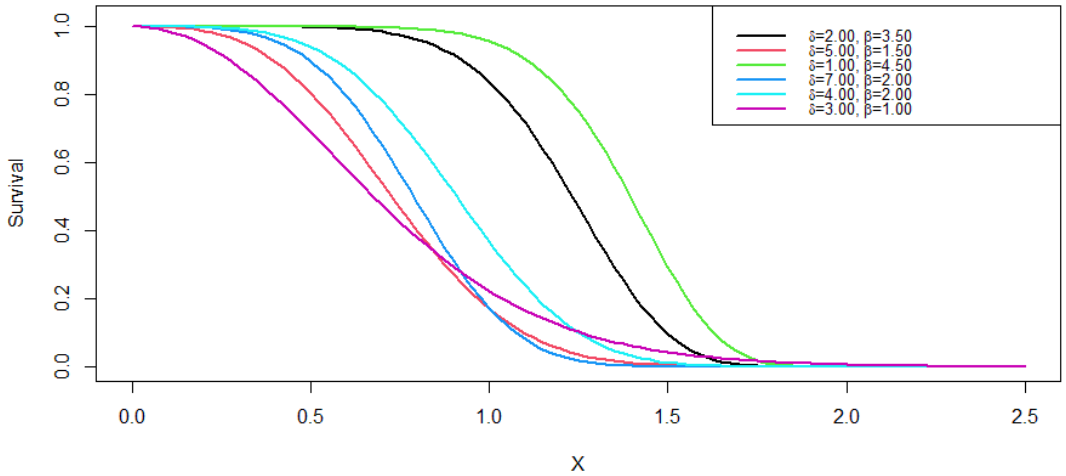

Figure 3. Plot Survival function for MWArctan distribution with different values of parameters

Figure 3 is the complement of the CDF and reflects the same behavior in reverse. Pairs with large δ decline earlier and with a pronounced slope, indicating shorter lifetimes and lower survival probability at small values of x. This is consistent with early pdf peaks and a rapid CDF crossing through half. This behavior is useful for reliability and failure times, because adjusting δ determines the timing of early risks, and adjusting β determines the severity of risks around the intermediate life and the shape of the tail later.

The hazard function $h(x)$ represents the instantaneous rate of failure at time x subject to survival until that time, and is given by [15], [16], [17]:

$$h(x) = \lim_{\Delta x \to \infty} \frac{P\left((x < X < x + \Delta x) \middle| X \geq x\right)}{\Delta x} = \frac{f(x)}{S(x)}$$

$$h(x) = \frac{4\delta\beta\, arctan(x)\left(2 - \frac{2}{\pi}arctan(x)\right)}{\pi^2\left(1 - \frac{2}{\pi}arctan(x)\right)^2(1 + x^2)}\left(\frac{\left(\frac{2}{\pi}arctan(x)\right)^2}{1 - \frac{2}{\pi}arctan(x)}\right)^{\beta-1}. \tag{10}$$

3.2 Expansion CDF and pdf of MWArctan distribution

The main goal of expansion is to rewrite complex functions in alternative forms (such as infinite series, elementary

functions, or integrals) to facilitate mathematical analysis, such as differentiation, integration, and finding statistical properties (such as mean and variance) that are difficult to calculate directly from the original form, which is the case for the MWArctan distribution. Starting with the expansion of the CDF function as follows:

Since

$$e^{-x} = \sum_{i=0}^{\infty} \frac{(-1)^i}{i!} x^i.$$

Then

$$e^{-\delta\left(\frac{\left(\frac{2}{\pi}arctan(x)\right)^2}{1-\frac{2}{\pi}arctan(x)}\right)^{\beta}} = \sum_{i=0}^{\infty} \frac{(-1)^i}{i!} \delta^i \frac{\left(\frac{2}{\pi}arctan(x)\right)^{2\beta i}}{\left(1-\frac{2}{\pi}arctan(x)\right)^{\beta i}},$$

and since

$$(1-x)^{-n} = \sum_{j=0}^{\infty} \frac{\Gamma(n+j)}{j!\,\Gamma(n)} x^j; \ \ |n| < 1, n > 0.$$

Then

$$\left(1-\frac{2}{\pi}arctan(x)\right)^{-\beta i} = \sum_{j=0}^{\infty} \frac{\Gamma(\beta i+j)}{j!\,\Gamma(\beta i)} \left(\frac{2}{\pi}arctan(x)\right)^j.$$

To get:

$$e^{-\delta\left(\frac{\left(\frac{2}{\pi}arctan(x)\right)^2}{1-\frac{2}{\pi}arctan(x)}\right)^{\beta}} = \sum_{i=0}^{\infty}\sum_{j=0}^{\infty} \frac{(-1)^i \Gamma(\beta i+j)}{i!\,j!\,\Gamma(\beta i)} \delta^i \left(\frac{2}{\pi}arctan(x)\right)^{2\beta i+j}$$

Hence a final form is:

$$G(x) = 1 - \mathfrak{X}\left(\frac{2}{\pi}arctan(x)\right)^{2\beta i+j}, \tag{11}$$

where $\mathfrak{X} = \sum_{i=0}^{\infty}\sum_{j=0}^{\infty} \frac{(-1)^i \Gamma(\beta i+j)}{i!\,j!\,\Gamma(\beta i)} \delta^i$.

The CDF^{α} has a form:

$$G^{\alpha}(x) = \left(1 - e^{-\delta\left(\frac{\left(\frac{2}{\pi}arctan(x)\right)^2}{1-\frac{2}{\pi}arctan(x)}\right)^{\beta}}\right)^{\alpha}. \tag{12}$$

Can be expanded as following: since $(1-\mathrm{t})^{\mathrm{a}} = \sum_{\mathrm{j}=0}^{\infty}(-1)^{\mathrm{j}} \binom{\mathrm{a}}{\mathrm{j}} \mathrm{t}^{\mathrm{j}}; \ |\mathrm{t}| < 1, \mathrm{a} > 0$, to get:

$$\left(1 - e^{-\delta\left(\frac{\left(\frac{2}{\pi}arctan(x)\right)^2}{1-\frac{2}{\pi}arctan(x)}\right)^{\beta}}\right)^{\alpha} = \sum_{k=0}^{\infty}(-1)^k \binom{\alpha}{k} e^{-\delta k\left(\frac{\left(\frac{2}{\pi}arctan(x)\right)^2}{1-\frac{2}{\pi}arctan(x)}\right)^{\beta}},$$

since $\mathrm{e}^{-\mathrm{x}} = \sum_{\mathrm{i}=0}^{\infty} \frac{(-1)^{\mathrm{i}}}{\mathrm{i}!} \mathrm{x}^{\mathrm{i}}$, then:

$$e^{-\delta k\left(\frac{\left(\frac{2}{\pi}arctan(x)\right)^2}{1-\frac{2}{\pi}arctan(x)}\right)^{\beta}} = \sum_{t=0}^{\infty} \frac{(-1)^t}{t!} \delta^t k^t \frac{\left(\frac{2}{\pi}arctan(x)\right)^{2t\beta}}{\left(1-\frac{2}{\pi}arctan(x)\right)^{t\beta}},$$

and $(1-\mathrm{x})^{-\mathrm{n}} = \sum_{\mathrm{j}=0}^{\infty} \frac{\Gamma(\mathrm{n}+\mathrm{j})}{\mathrm{j}!\Gamma(\mathrm{n})} \mathrm{x}^{\mathrm{j}}; \ |\mathrm{n}| < 1, \mathrm{n} > 0$, we get:

$$\left(1-\frac{2}{\pi}arctan(x)\right)^{-t\beta}=\sum_{s=0}^{\infty}\frac{\Gamma(t\beta+s)}{s!\,\Gamma(t\beta)}\left(\frac{2}{\pi}arctan(x)\right)^{s}.$$

To get a final expansion form:

$$G^{\alpha}(x)=\mathcal{W}\left(\frac{2}{\pi}arctan(x)\right)^{2t\beta+s}, \tag{13}$$

where $\mathcal{W}=\sum_{k=0}^{\infty}\sum_{t=0}^{\infty}\sum_{s=0}^{\infty}\frac{(-1)^{k+t}\Gamma(t\beta+s)}{t!s!\Gamma(t\beta)}\binom{\alpha}{k}\delta^{t}k^{t}$.

By same way in to expand CDF and CDF$^{\alpha}$ can be expand the pdf to get a pdf expand form:

$$g(x)=\mathbb{A}\left(\frac{2}{\pi}arctan(x)\right)^{2\beta(i+1)+z-1}\frac{\left(2-\frac{2}{\pi}arctan(x)\right)}{(1+x^{2})}, \tag{14}$$

where $\mathbb{A}=\sum_{i=0}^{\infty}\sum_{z=0}^{\infty}\frac{(-1)^{i}\Gamma\{\beta(i+1)+1+z\}}{\pi i!z!\Gamma(z)\delta^{-(i+1)}}2\beta$.

3.3 Moment function of MWArctan distribution

In mathematical statistics and probability theory, there is no independent entity called a "moment function" Instead, the term "moments" refers to a family of numerical values that describe important properties of the probability distribution of a random variable. These are numerical coefficients that summarize the shape, position, and spread of the probability distribution curve. The function's mission is precisely to provide a systematic way to calculate all these moments from a single function. The moment of order n about the origin of a random variable X is defined as the expected value of the n-power of the variable, and defined by form [18], [19], [20]:

$$\mu_{n}=E(x^{n})=\int_{-\infty}^{\infty}x^{n}g(x)dx=\mathbb{A}\left(\frac{2}{\pi}arctan(x)\right)^{2\beta(i+1)+z-1}\frac{\left(2-\frac{2}{\pi}arctan(x)\right)}{(1+x^{2})}.$$

The moment for MWArctan distribution can be founded by substitute Equation (14) in above equation to get a form:

$$\mu_{n}=2\mathbb{A}\int_{0}^{\infty}x^{n}\left(\frac{2}{\pi}arctan(x)\right)^{\gamma}\frac{\left(1-\frac{1}{\pi}arctan(x)\right)}{(1+x^{2})}dx,$$

where $\gamma=2\beta(i+1)+z-1$.

Let $u=arctan(x)\Longrightarrow x=tan(u)\Longrightarrow dx=\frac{du}{1-tan^{2}(u)}=\cos^{2}(u)\,du$

But $\frac{dx}{1+x^{2}}=du$

Also, when $x=0\Longrightarrow u=0, x=\infty\Longrightarrow u=\frac{\pi}{2}$

Then we get: $x^{n}=tan^{n}(u)$, $\frac{2}{\pi}arctan(x)=\frac{2}{\pi}u$, and $1-\frac{1}{\pi}arctan(x)=1-\frac{u}{\pi}$

$$\mu_{n}=\mathbb{A}\frac{2^{\alpha+1}}{\pi^{\alpha}}\int_{0}^{\infty}tan^{n}(u)\,u^{\gamma}\left(1-\frac{u}{\pi}\right)du$$

$$\mu_{n}=\mathbb{A}\frac{2^{\alpha+1}}{\pi^{\alpha}}\left\{\int_{0}^{\frac{\pi}{2}}tan^{n}(u)\,u^{\gamma}du-\frac{1}{\pi}\int_{0}^{\frac{\pi}{2}}tan^{n}(u)\,u^{\gamma+1}du\right\}$$

Set $v=\frac{2u}{\pi},\Longrightarrow u=\frac{\pi v}{2}\Longrightarrow du=\frac{\pi}{2}dv, v\in[0,1]$

$$\mu_{n}=\mathbb{A}\frac{\pi}{2}\int_{0}^{1}v^{\gamma}(2-v)\,tan^{n}\left(\frac{\pi v}{2}\right)dv$$

Notice that

$$f(v)=\frac{v^{\gamma}(1-v)}{Beta(\gamma+1,2)}\quad,\quad v\in[0,1],$$

where $Beta(\gamma+1,2)$ is density beta random variable U, such that $U\sim Beta(\gamma+1,2)=\frac{1}{(\gamma+1)(\gamma+2)}$, then we get:

$$\mu_{n}=\frac{\pi\mathbb{A}}{2(\gamma+1)(\gamma+2)}E_{U\sim Beta(\gamma+1,2)}\left(\frac{2-U}{1-U}tan^{n}(U)\right). \tag{15}$$

3.4 Quantile function of MWArctan distribution

The quantile function, also known as the piecewise function, is a fundamental concept in introductory and nonparametric statistics. It can be precisely defined as follows [21], [22]:

Let X be any random variable with a CDF is $F(x) = P(X \leq x)$. The quantile function $Q(q)$ is defined as the inverse of the CDF. Mathematically, it is defined for any probability q (where $0 < q < 1$) as: $Q(q) = F^{-1}(q) = inf\{x \in R: F_X(x) \geq q\}$. Therefore, $Q(q)$ is the smallest value of x for which the cumulative distribution $F(x)$ is at least equal to the probability q. then the quantile function of MWArctan distribution can be founded by put:

$$q = 1 - e^{-\delta\left(\frac{\left(\frac{2}{\pi}arctan(x)\right)^2}{1-\frac{2}{\pi}arctan(x)}\right)^{\beta}}$$

$$q = 1 - e^{-\delta\left(\frac{\left(\frac{2}{\pi}arctan(x)\right)^2}{1-\frac{2}{\pi}arctan(x)}\right)^{\beta}}$$

$$1 - q = e^{-\delta\left(\frac{\left(\frac{2}{\pi}arctan(x)\right)^2}{1-\frac{2}{\pi}arctan(x)}\right)^{\beta}}$$

$$-\frac{\ln(1-q)}{\delta} = \left(\frac{\left(\frac{2}{\pi}arctan(x)\right)^2}{1-\frac{2}{\pi}arctan(x)}\right)^{\beta}$$

$$\left\{-\frac{\ln(1-q)}{\delta}\right\}^{\frac{1}{\beta}} = \frac{\left(\frac{2}{\pi}arctan(x)\right)^2}{1-\frac{2}{\pi}arctan(x)}$$

$$\left\{-\frac{\ln(1-q)}{\delta}\right\}^{\frac{1}{\beta}}\left(1-\frac{2}{\pi}arctan(x)\right) = \left(\frac{2}{\pi}arctan(x)\right)^2$$

But $k = \left\{-\frac{\ln(1-q)}{\delta}\right\}^{\frac{1}{\beta}}$

$$k\left(1-\frac{2}{\pi}arctan(x)\right) = \left(\frac{2}{\pi}arctan(x)\right)^2$$

$$\left(\frac{2}{\pi}arctan(x)\right)^2 + k\frac{2}{\pi}arctan(x) - k = 0$$

$$\frac{2}{\pi}arctan(x) = \frac{-k \mp \sqrt{k^2 - 4k}}{2}$$

$$arctan(x) = \pi\frac{-k \mp \sqrt{k^2 - 4k}}{4}$$

Hence we get:

$$x = \tan\left(\pi\frac{-k \mp \sqrt{k^2 - 4k}}{4}\right)$$

Or

$$Q(x) = Q_q\left(\tan\left(\pi\frac{-\left\{-\frac{\ln(1-q)}{\delta}\right\}^{\frac{1}{\beta}} \mp \sqrt{\left\{-\frac{\ln(1-q)}{\delta}\right\}^{\frac{2}{\beta}} - 4\left\{-\frac{\ln(1-q)}{\delta}\right\}^{\frac{1}{\beta}}}}{4}\right)\right). \quad (16)$$

Table 1 displays the quantile function values for the MWArctan distribution under various parameters (δ, β). The table shows the quantile values at selected probability levels ($u = 0.125, 0.250, 0.375, 0.500, 0.625, 0.750$, and 0.875), which are the points below which a given portion of the data falls. The table includes five parameter combinations.

Table 1: Explanation of the Quantile function for MWArctan distribution

q	(δ, β)				
	(2.2,1.7)	(1.6,2.8)	(2.3,0.9)	(1.9,3.3)	(2,2.8)
0.125	0.6189987	0.9044612	0.3001519	0.9436321	0.8683346
0.250	0.7731986	1.0431397	0.4502865	1.0659309	1.0003294
0.375	0.8947539	1.1455507	0.5850569	1.1543913	1.0975372
0.500	1.0072326	1.2355546	0.7226117	1.2309576	1.1828230
0.625	1.1225357	1.3235862	0.8770888	1.3047954	1.2661159
0.750	1.2541424	1.4194085	1.0713531	1.3840786	1.3566603
0.875	1.4341556	1.5433076	1.3712102	1.4849736	1.4734932

The results of Table 1 show a clear upward trend in quantile values as u increases, confirming the monotonic property of the quantile function. For example, when comparing the effect of the parameters, we note that small values of β lead to lower quantile values at the same probability level, reflecting a more left-tailed distribution. Large values of β, on the other hand, raise the quantile values more rapidly, indicating a heavier right tail. Thus, the table shows how the parameters affect the shape and spread of the MWArctan distribution, highlighting its flexibility in representing data with different patterns of skewness and kurtosis.

The measurements of skewness (S) and kurtosis (K) based on Quantile function were defined as follows [23], [24]:

$$S = \frac{Q(0.750) - 2Q(0.500) + Q(0.250)}{Q(0.750) - Q(0.250)}, \tag{17}$$

$$K = \frac{Q(875) - Q(0.625) + Q(0.375) - Q(0.125)}{Q(0.750) - Q(0.250)}. \tag{18}$$

From Table 1 the skewness and kurtosis for all cases have a following value:

Case 1	$S = 0.026772$ $K = 1.221297$
Case 2	$S = -0.022752$ $K = 1.224685$
Case 3	$S = 0.123040$ $K = 1.254336$
Case 4	$S = -0.037422$ $K = 1.228792$
Case 5	$S = -0.024293$ $K = 1.225209$

From the above values it is clear that the distribution generates a slight right or left skew with the thickness of the edges being almost constant across the cases.

4. Estimation

Maximum Likelihood Estimation (MLE) is the most popular and widely used estimation method due to its wide acceptance in a very large body of research and also because it is easy to find compared to other methods. Suppose $X_1, X_2, \dots, X_n$ are random samples of size n from the MWArctan distribution with unknown parameters (δ, β) defined in advance. The maximum likelihood function will be [25], [26]:

$$L(\Theta, X) = \prod_{i=1}^{n} g(x_i; \Theta), \qquad \Theta = (\delta, \beta). \tag{19}$$

By substituting pdf function for MWArctan distribution of Equation (8) in Equation (19) to get a form:

$$L = \prod_{i=1}^{n} 4\delta\beta e^{-\delta\left(\frac{\left(\frac{2}{\pi}arctan(x_i)\right)^2}{1-\frac{2}{\pi}arctan(x_i)}\right)^{\beta}} \left(\frac{\left(\frac{2}{\pi}arctan(x_i)\right)^2}{1-\frac{2}{\pi}arctan(x_i)}\right)^{\beta-1} \frac{arctan(x_i)\left(2-\frac{2}{\pi}arctan(x_i)\right)}{\pi^2\left(1-\frac{2}{\pi}arctan(x_i)\right)^2\left(1+x_i^2\right)}. \tag{20}$$

Take normal logarithm for Equation (20) to get:

$$L = n\ln 4 + n\ln\delta + n\ln\beta - \delta\sum_{i=0}^{n} A_i^{\beta} + (\beta - 1)\sum_{i=0}^{n}\ln(A_i) + \sum_{i=0}^{n} C_i, \qquad (21)$$

where $A_i = \frac{\left(\frac{2}{\pi}arctan(x_i)\right)^2}{1-\frac{2}{\pi}arctan(x_i)}$, and $C_i = \ln(arctan(x_i)) + \ln\left(2 - \frac{2}{\pi}arctan(x_i)\right) - 2\ln(\pi) - 2\ln\left(1 - \frac{2}{\pi}arctan(x_i)\right) - \ln(1 + x_i^2)$.

Then by derivative Equation (21) to δ and β to get:

$$\frac{\partial L}{\partial \delta} = \frac{n}{\delta} - \sum_{i=0}^{n} A_i^{\beta},$$

$$\frac{\partial L}{\partial \beta} = \frac{n}{\beta} - \delta\sum_{i=0}^{n} A_i^{\beta}\ln(A_i) + \sum_{i=0}^{n}\ln(A_i).$$

Closed-form update for δ given β

$$\hat{\delta}(\beta) = \frac{n}{\sum_{i=0}^{n} A_i^{\beta}}.$$

Single-equation in β after plugging $\hat{\delta}(\beta)$:

$$0 = \frac{n}{\beta} - n\frac{\sum_{i=0}^{n} A_i^{\beta}\ln(A_i)}{\sum_{i=0}^{n} A_i^{\beta}} + \sum_{i=0}^{n}\ln(A_i).$$

Solve numerically for $\hat{\beta}$, then set $\hat{\delta} = \hat{\delta}(\hat{\beta})$. Hessian (for joint Newton or standard errors)

$$\frac{\partial^2 L}{\partial \delta^2} = -\frac{n}{\delta^2},$$

$$\frac{\partial^2 L}{\partial \beta^2} = -\frac{n}{\beta^2} - \delta\sum_{i=0}^{n} A_i^{\beta}\{\ln(A_i)\}^2,$$

$$\frac{\partial^2 L}{\partial \delta \partial \beta} = -\sum_{i=0}^{n} A_i^{\beta}\ln(A_i).$$

Least squares estimation (LSE) is done by choosing the values that minimize the sum of squares of the differences between the observed values and the model output and is given by the equation below [27], [14], [28]:

$$\varphi(\vartheta) = \sum_{i=1}^{m}\left[G(x_i) - \frac{i}{n+1}\right]^2,$$

$$\varphi(\vartheta) = \sum_{i=1}^{m}\left[1 - e^{-\delta\left(\frac{\left(\frac{2}{\pi}arctan(x_i)\right)^2}{1-\frac{2}{\pi}arctan(x_i)}\right)^{\beta}} - \frac{i}{n+1}\right]^2. \qquad (22)$$

Weighted Least squares estimation (WLSE) is done by choosing the values that minimize the sum of squares of the differences between the observed values and the model output with adding weight (Similar to LSE but with added weight to the function) and is given by the equation below [10], [29]:

$$W(\vartheta) = \sum_{i=1}^{m} W_i\left[G(x_i) - \frac{i}{n+1}\right]^2,$$

$$W(\vartheta) = \sum_{i=1}^{m} W_i\left[1 - e^{-\delta\left(\frac{\left(\frac{2}{\pi}arctan(x_i)\right)^2}{1-\frac{2}{\pi}arctan(x_i)}\right)^{\beta}} - \frac{i}{n+1}\right]^2. \qquad (23)$$

5. Simulation

A comprehensive Monte Carlo simulation study was conducted to evaluate the performance of the finite sample characteristics of three different estimation methods: MLE, LSE, and WLSE, in estimating the shape (β) and scale (δ) parameters of the MWArct distribution. The simulations were performed for two different levels of true parameter values and a wide range of sample sizes (N) ranging from 20 to 500, with a large number of iterations (4000) to ensure the reliability of the results. Performance was measured using four main statistical measures: mean estimates (Mean) [30], [29], bias (Bias) [31], [28], mean square error (MSE) [32], [33], and root mean square error (RMSE) [34], [35].

Table 2: Monte Carlo simulation of MWArctan distribution where $\delta = 2.9, \beta = 2.1$

Est.	Ess. Par.	$N = 20$			$N = 40$		
		MLE	**LSE**	**WLSE**	**MLE**	**LSE**	**WLSE**
Mean	$\hat{\delta}$	3.3038298	3.0679893	3.0897609	3.0662717	2.94713065	2.96956655
	$\hat{\beta}$	2.2575962	2.08926501	2.11280219	2.17222282	2.09308989	2.11139148
MSE	$\hat{\delta}$	1.3803590	5.6633163	4.7778604	0.4068573	0.63047420	0.52222413
	$\hat{\beta}$	0.2088959	0.24653453	0.22161075	0.08415180	0.11386231	0.09721603
RMSE	$\hat{\delta}$	1.1748868	2.3797723	2.1858318	0.6378537	0.79402406	0.72265077
	$\hat{\beta}$	0.4570513	0.49652244	0.47075551	0.29008929	0.33743490	0.31179486
Bias	$\hat{\delta}$	0.4038298	0.1679893	0.1897609	0.1662717	0.04713065	0.06956655
	$\hat{\beta}$	0.1575962	0.01073499	0.01280219	0.07222282	0.00691010	0.01139148
Est.	**Ess. Par.**	$N = 100$			$N = 150$		
		MLE	**LSE**	**WLSE**	**MLE**	**LSE**	**WLSE**
Mean	$\hat{\delta}$	2.97602314	2.92205335	2.94051377	2.93806467	2.90711229	2.91979952
	$\hat{\beta}$	2.13250906	2.09884812	2.11124217	2.12096942	2.09929554	2.10870052
MSE	$\hat{\delta}$	0.12753336	0.16850933	0.14062127	0.07864686	0.11365191	0.09231051
	$\hat{\beta}$	0.03032009	0.04156276	0.03439618	0.01885777	0.02721653	0.02224460
RMSE	$\hat{\delta}$	0.35711814	0.41049888	0.37499503	0.28044047	0.33712298	0.30382644
	$\hat{\beta}$	0.17412666	0.20386946	0.18546206	0.13732358	0.16497434	0.14914626
Bias	$\hat{\delta}$	0.07602314	0.02205335	0.04051377	0.03806467	0.00711229	0.01979952
	$\hat{\beta}$	0.03250906	0.00115187	0.01124217	0.02096942	0.00070445	0.00870052
Est.	**Ess. Par.**	$N = 200$			$N = 300$		
		MLE	**LSE**	**WLSE**	**MLE**	**LSE**	**WLSE**
Mean	$\hat{\delta}$	2.93457593	2.91256044	2.92142243	2.92064365	2.90229401	2.91051317
	$\hat{\beta}$	2.11442918	2.09973577	2.10634303	2.10981479	2.09805558	2.10347861
MSE	$\hat{\delta}$	0.05740656	0.08222485	0.06571842	0.03626660	0.05290299	0.04206322
	$\hat{\beta}$	0.01394798	0.02034188	0.01623489	0.00940404	0.01347386	0.01084048
RMSE	$\hat{\delta}$	0.23959666	0.28674875	0.25635604	0.19043791	0.23000650	0.20509321
	$\hat{\beta}$	0.11810157	0.14262499	0.12741622	0.09697445	0.11607696	0.10411761
Bias	$\hat{\delta}$	0.03457593	0.01256044	0.02142243	0.02064365	0.00229401	0.01051317
	$\hat{\beta}$	0.01442918	0.00026422	0.00634303	0.00981479	0.00194441	0.00347861
Est.	**Ess. Par.**	$N = 400$			$N = 500$		
		MLE	**LSE**	**WLSE**	**MLE**	**LSE**	**WLSE**
Mean	$\hat{\delta}$	2.91271008	2.90335343	2.90882557	2.91030716	2.90097567	2.90550428
	$\hat{\beta}$	2.10709747	2.10043281	2.10431284	2.10399345	2.09781537	2.10091278
MSE	$\hat{\delta}$	0.02617099	0.03881298	0.03064868	0.02192086	0.03180792	0.02540277
	$\hat{\beta}$	0.00676124	0.01017046	0.00807345	0.00548726	0.00808315	0.00645381
RMSE	$\hat{\delta}$	0.16177451	0.19701011	0.17506766	0.14805696	0.17834775	0.15938248
	$\hat{\beta}$	0.08222679	0.10084870	0.08985239	0.07407606	0.08990638	0.08033560
Bias	$\hat{\delta}$	0.01271008	0.00335343	0.00882557	0.01030716	0.00097567	0.00550428
	$\hat{\beta}$	0.00709747	0.00043281	0.00431284	0.00399345	0.00218462	0.00091278

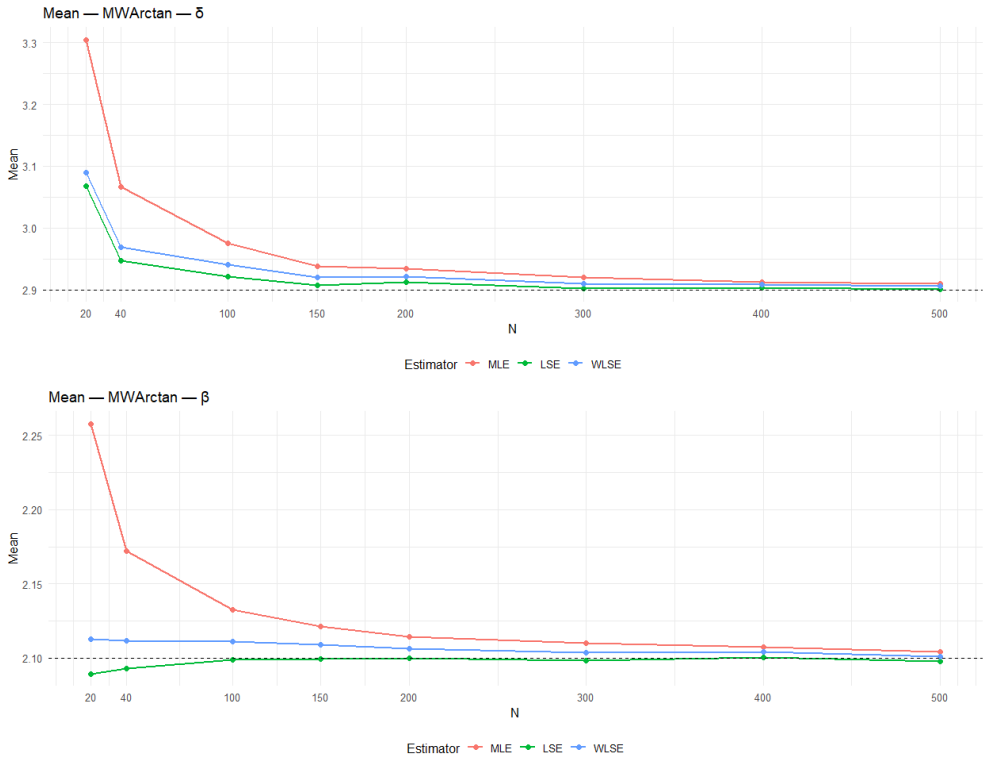

Figure 4. Mean trends values for simulation

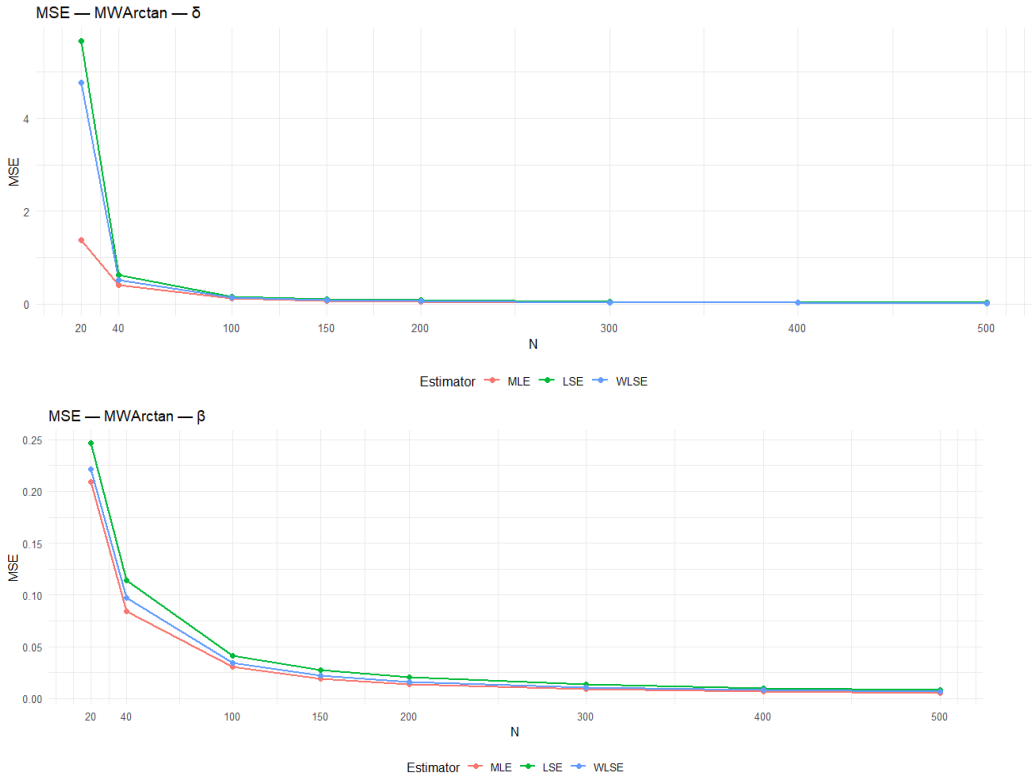

Figure 5. MSE trends values for simulation

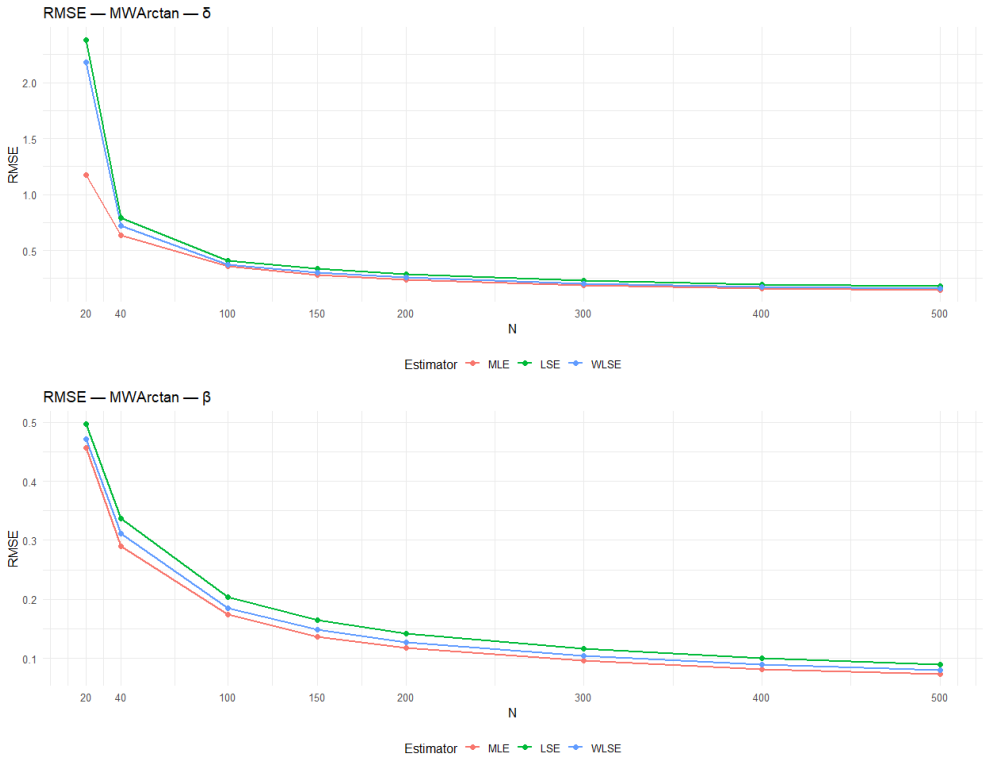

Figure 6. RMSE trends values for simulation

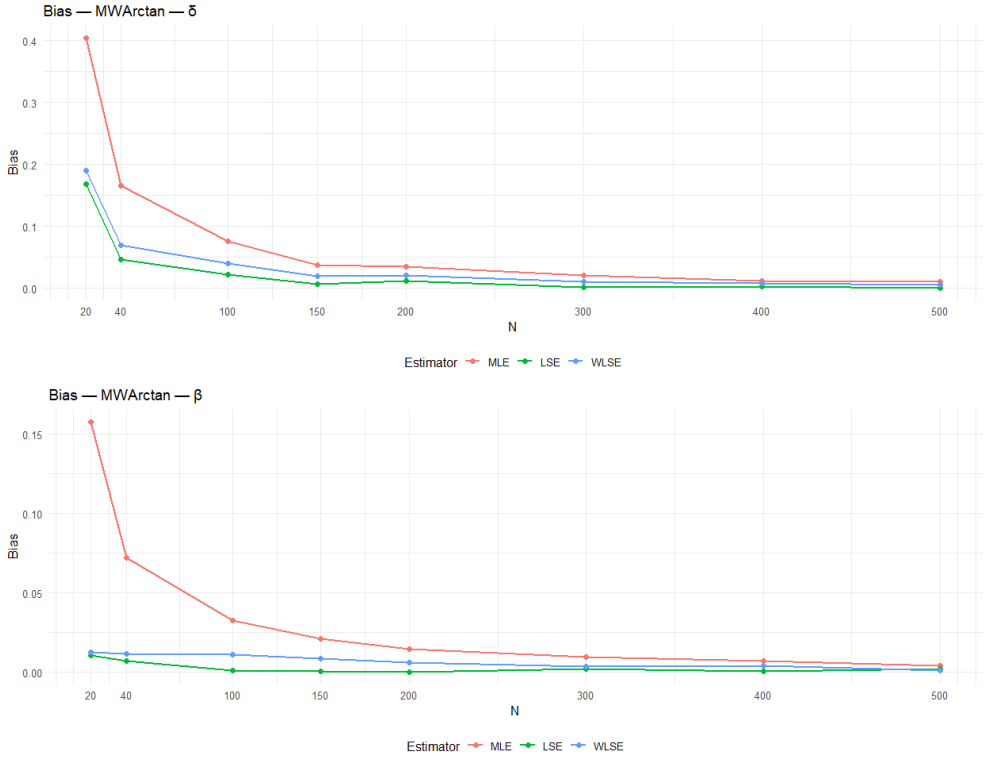

Figure 7. Bias trends values for simulation

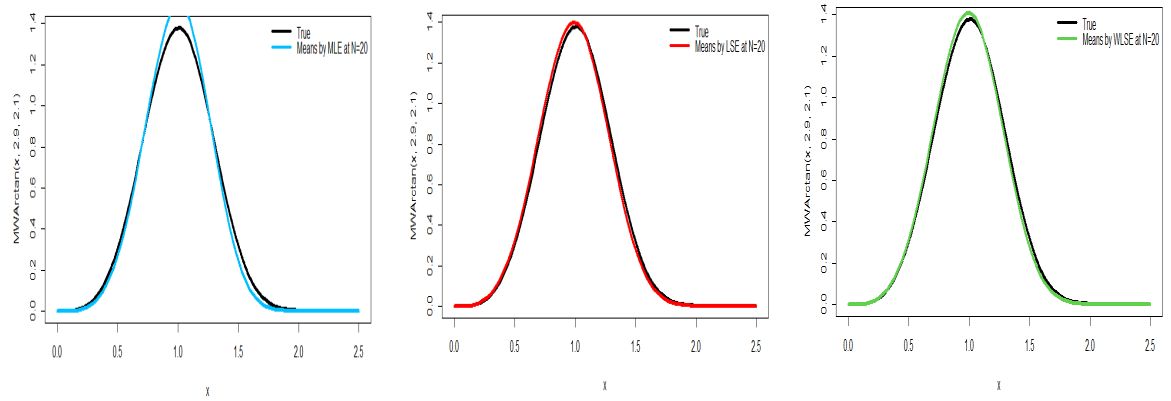

$N = 20$

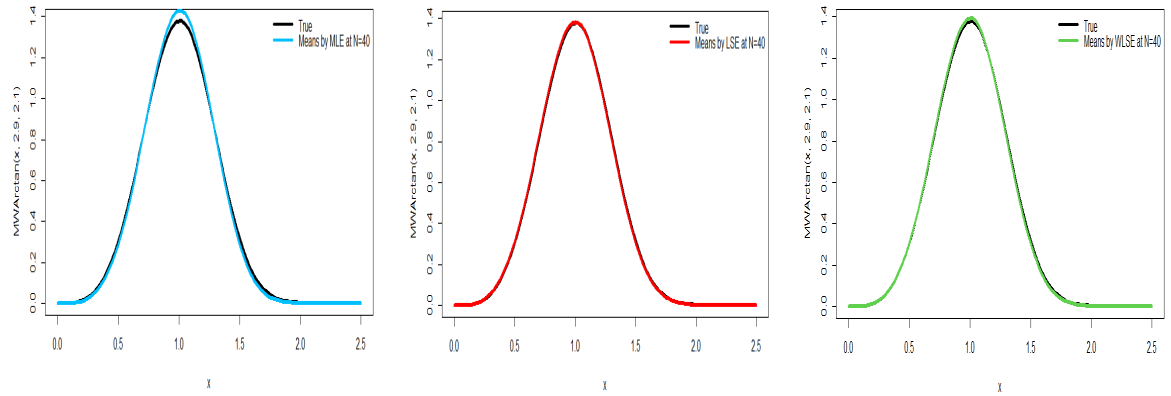

$N = 40$

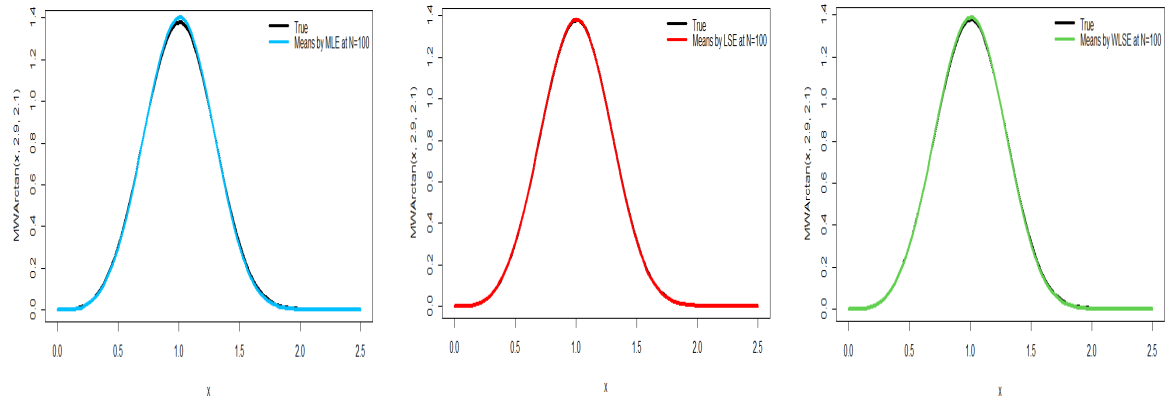

$N = 100$

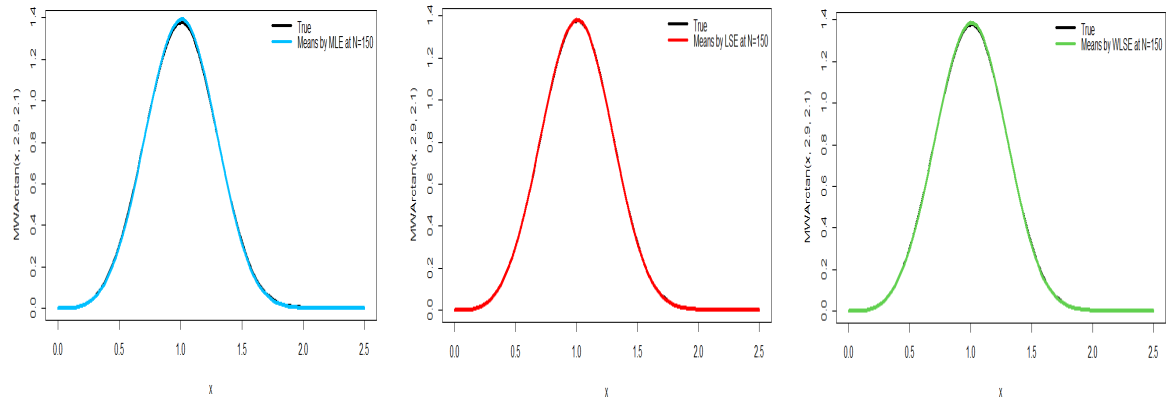

$N = 150$

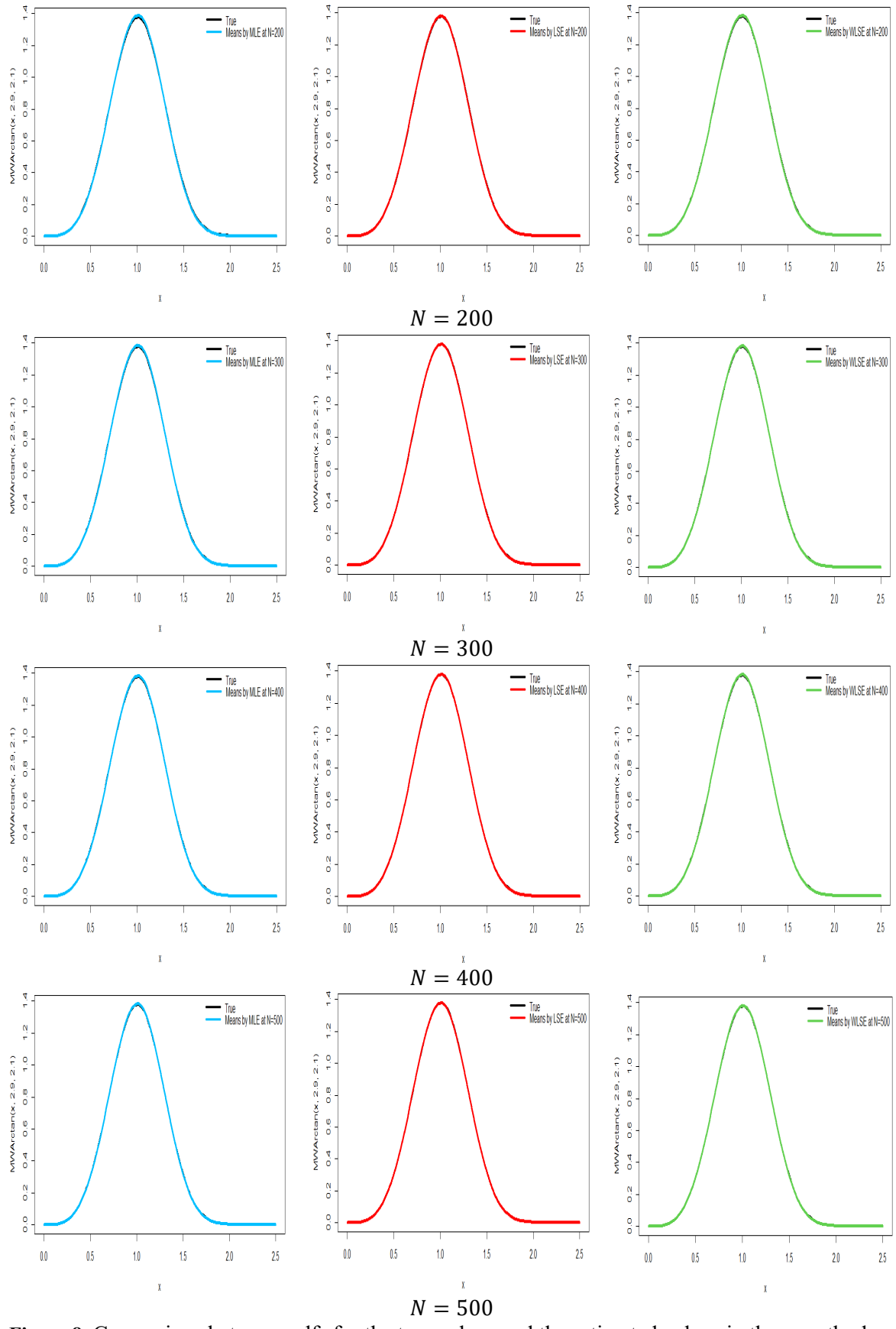

Figure 8. Comparison between pdfs for the true values and the estimated values in three methods for the sample sizes of the simulation table, case 1

Analysis of the results reveals a more accurate performance picture. While the MLE outperforms in overall accuracy (low MSE), as shown in Table 3 and Figure 5, the LSE method emerges as the least biased estimator for most sample sizes,

particularly for the β parameter.

Analyzing the results in Table 2 and the graphs in Figures 4 to 8 shows that all parameter estimators exhibited statistical consistency. This is evident in the mean values of the estimates (means) approaching the true values of the parameters (2.9 and 2.1, respectively) as the sample size increases, as shown in the trend curves in Figure 4.

In terms of accuracy, the MLE recorded the MSE and RMSE values across almost all sample sizes, as shown in Table 3 and visually demonstrated by the steeper downward trend of its MSE and RMSE curves in Figures 5 and 6, respectively. This indicates that MLE is superior in terms of overall accuracy (which includes variance and bias) compared to the LSE and WLSE methods.

Regarding bias, all methods showed a small and decreasing bias as the sample size increased (Figure 7). Although the LSE estimator sometimes showed less bias than the MLE in small samples (e.g., N=20), this slight improvement in impartiality comes at the cost of a significant variance inflation, as evidenced by the higher MSE values for LSE compared to MLE. Therefore, the MLE estimator remains superior according to the MSE criterion, which gives a balanced weight to bias and variance.

Finally, Figure 8 confirms these results numerically by visually comparing the density function curve (pdf) using the true values with the density curves using the average estimates. The comparison shows a steady and rapid convergence of the MLE-estimated curves toward the true curve as the sample size increases, reinforcing the conclusion of its superiority.

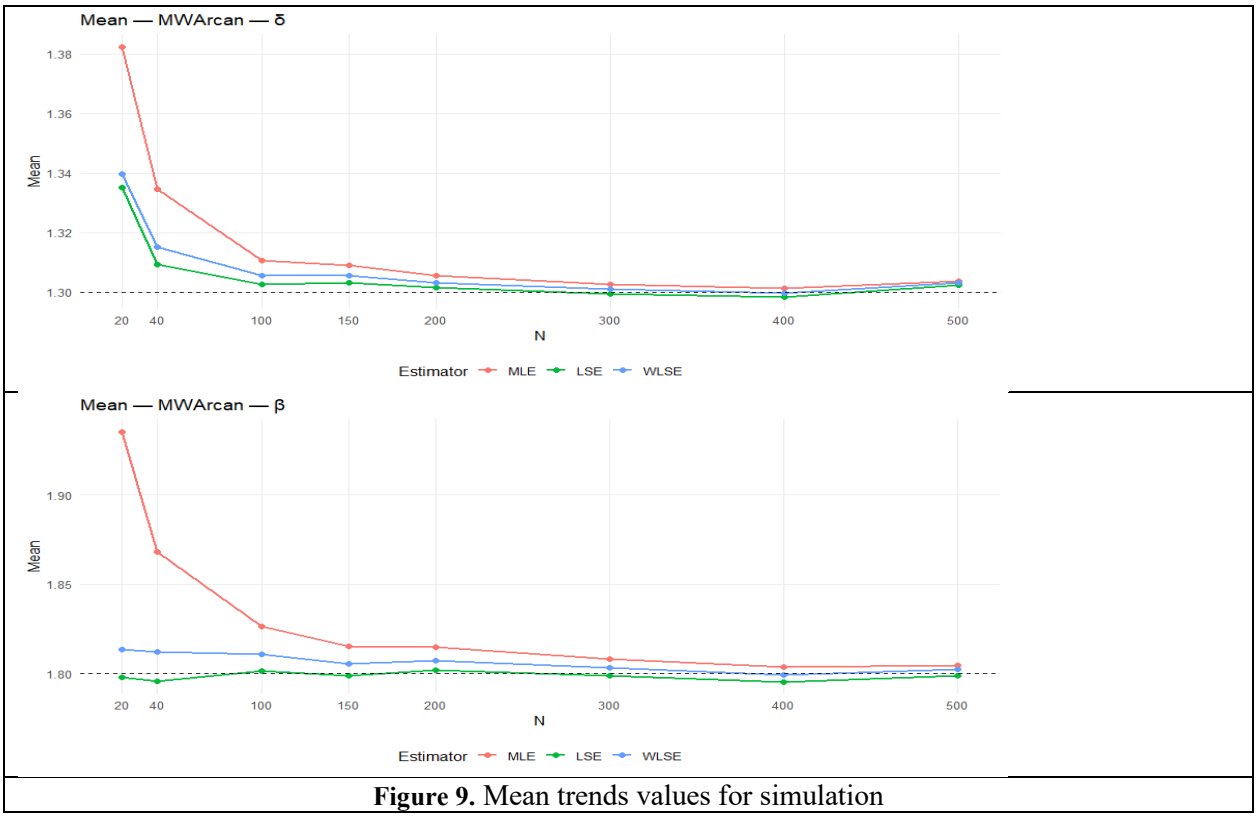

Figure 9. Mean trends values for simulation

Table 3: Monte Carlo simulation of MWArcan distribution where $\delta = 1.3, \beta = 1.8$

Est.	Ess. Par.	$N = 20$			$N = 40$		
		MLE	**LSE**	**WLSE**	**MLE**	**LSE**	**WLSE**
Mean	$\hat{\delta}$	1.38233301	1.33518308	1.33977184	1.33468719	1.309151514	1.31504322
	$\hat{\beta}$	1.9350866	1.79781975	1.81366991	1.86829529	1.795568456	1.81208179
MSE	$\hat{\delta}$	0.14146076	0.15753285	0.14466730	0.05243627	0.057483697	0.05333323
	$\hat{\beta}$	0.1531613	0.18411428	0.16441807	0.06426680	0.080094730	0.06895977
RMSE	$\hat{\delta}$	0.37611270	0.39690409	0.38035155	0.22898967	0.239757580	0.23093989
	$\hat{\beta}$	0.3913583	0.42908540	0.40548499	0.25350898	0.283010124	0.26260193
Bias	$\hat{\delta}$	0.08233301	0.03518308	0.03977184	0.03468719	0.009151514	0.01504322
	$\hat{\beta}$	0.1350866	0.00218025	0.01366991	0.06829529	0.004431544	0.01208179
Est.	**Ess. Par.**	$N = 100$			$N = 150$		
		MLE	**LSE**	**WLSE**	**MLE**	**LSE**	**WLSE**
Mean	$\hat{\delta}$	1.31046198	1.302464246	1.30537397	1.30906731	1.303131594	1.305531224
	$\hat{\beta}$	1.82632484	1.801585325	1.81061510	1.81547067	1.798882243	1.805527027
MSE	$\hat{\delta}$	0.01872888	0.021312836	0.01957177	0.01164783	0.013635917	0.012377213
	$\hat{\beta}$	0.02227586	0.031442057	0.02601032	0.01358102	0.019819880	0.016046892
RMSE	$\hat{\delta}$	0.13685350	0.145989163	0.13989914	0.10792513	0.116772931	0.111252924
	$\hat{\beta}$	0.14925099	0.177319082	0.16127716	0.11653764	0.140783096	0.126676327
Bias	$\hat{\delta}$	0.01046198	0.002464246	0.00537397	0.00906731	0.003131594	0.005531224
	$\hat{\beta}$	0.02632484	0.001585325	0.01061510	0.01547067	0.001117757	0.005527027
Est.	**Ess. Par.**	$N = 200$			$N = 300$		
		MLE	**LSE**	**WLSE**	**MLE**	**LSE**	**WLSE**
Mean	$\hat{\delta}$	1.305403316	1.301496393	1.303125938	1.302564100	1.2993968912	1.3008656257
	$\hat{\beta}$	1.81491016	1.801869605	1.807437731	1.808008628	1.798628516	1.803200819
MSE	$\hat{\delta}$	0.008699911	0.010006280	0.009145048	0.005713427	0.0065302520	0.0059663853
	$\hat{\beta}$	0.01042213	0.015030290	0.012215428	0.006765853	0.009469924	0.007682857
RMSE	$\hat{\delta}$	0.093273316	0.100031397	0.095629744	0.075587212	0.0808099748	0.0772423802
	$\hat{\beta}$	0.10208886	0.122598083	0.110523428	0.082254804	0.097313536	0.087651908
Bias	$\hat{\delta}$	0.005403316	0.001496393	0.003125938	0.002564100	0.0006031088	0.0008656257
	$\hat{\beta}$	0.01491016	0.001869605	0.007437731	0.008008628	0.001371484	0.003200819
Est.	**Ess. Par.**	$N = 400$			$N = 500$		
		MLE	**LSE**	**WLSE**	**MLE**	**LSE**	**WLSE**
Mean	$\hat{\delta}$	1.301312865	1.298366795	1.2997568126	1.303682102	1.302248386	1.303140313
	$\hat{\beta}$	1.803715570	1.795405618	1.7994320085	1.804672354	1.7990136468	1.802243022
MSE	$\hat{\delta}$	0.004479881	0.005030953	0.0046406550	0.003487917	0.004078990	0.003674403
	$\hat{\beta}$	0.004869298	0.007396843	0.0058732769	0.004129307	0.0059878580	0.004821756
RMSE	$\hat{\delta}$	0.066931915	0.070929214	0.0681223532	0.059058590	0.063866971	0.060616850
	$\hat{\beta}$	0.069780357	0.086004901	0.0766373078	0.064259686	0.0773812512	0.069438863
Bias	$\hat{\delta}$	0.001312865	0.001633205	0.0002431874	0.003682102	0.002248386	0.003140313
	$\hat{\beta}$	0.003715570	0.004594382	0.0005679915	0.004672354	0.0009863532	0.002243022

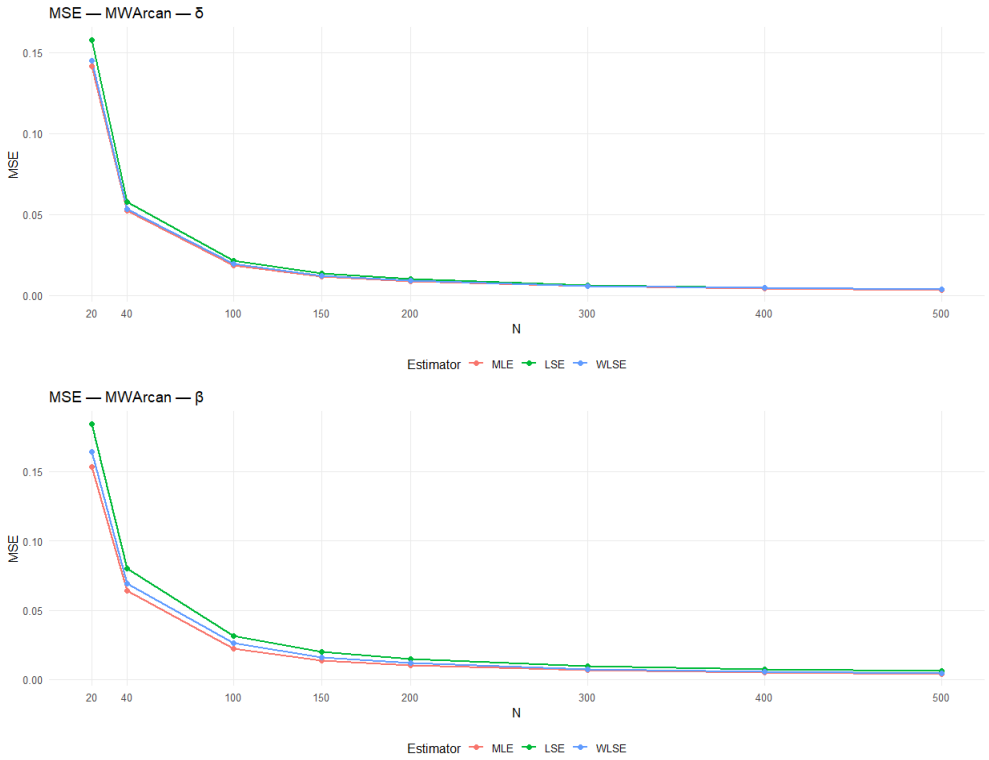

Figure 10. MSE trends values for simulation

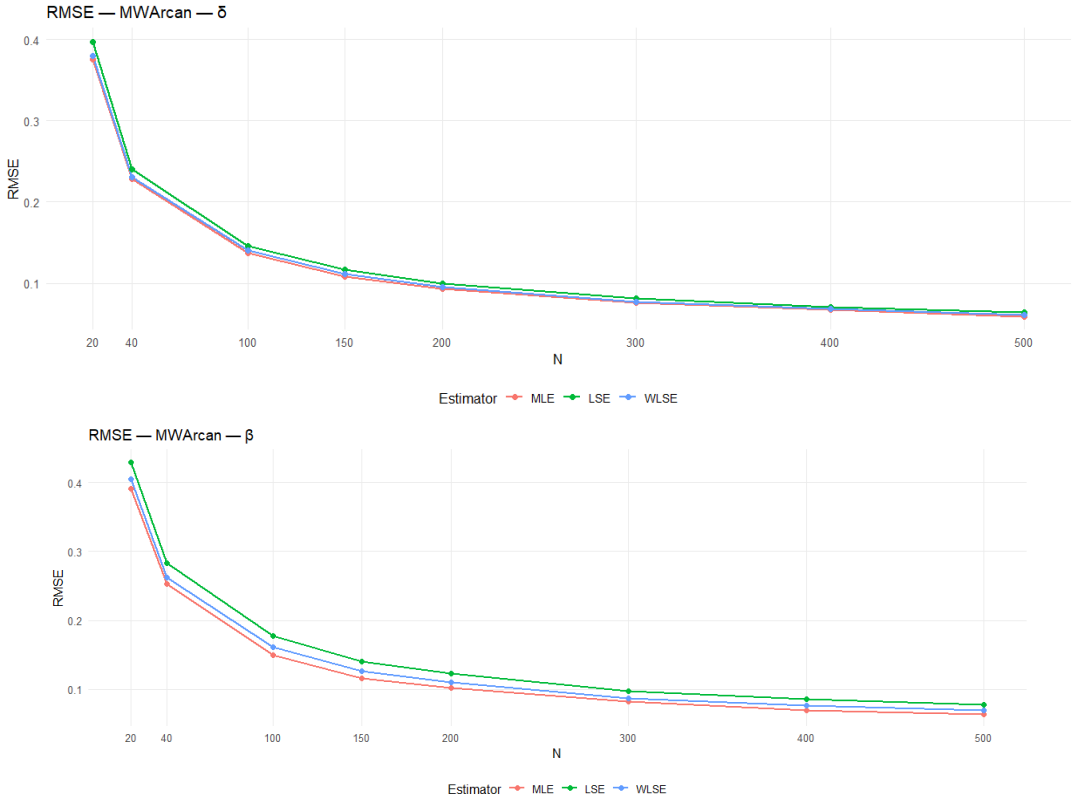

Figure 11. RMSE trends values for simulation

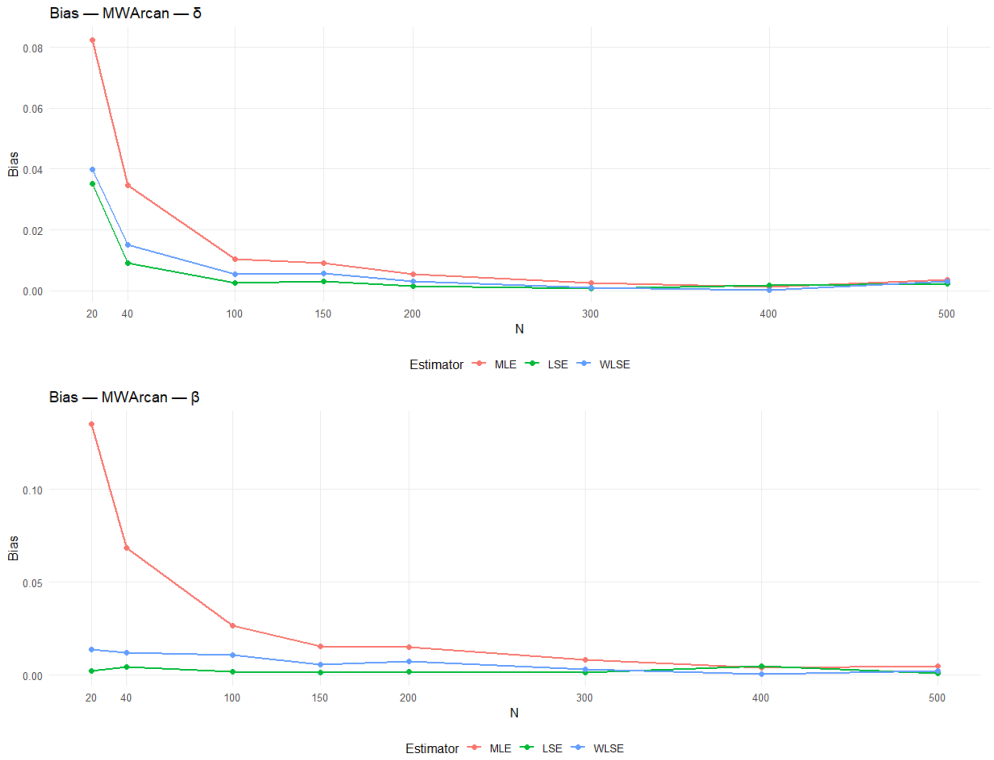

Figure 12. Bias trends values for simulation

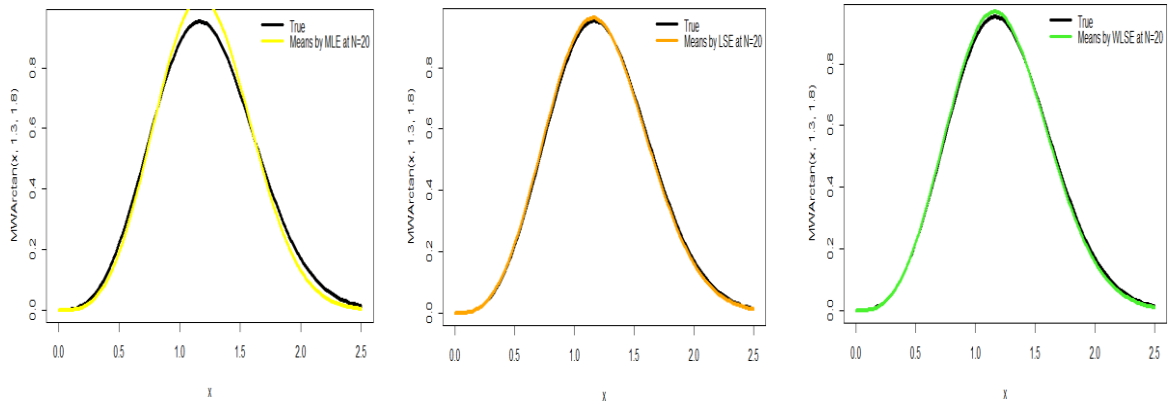

$N = 20$

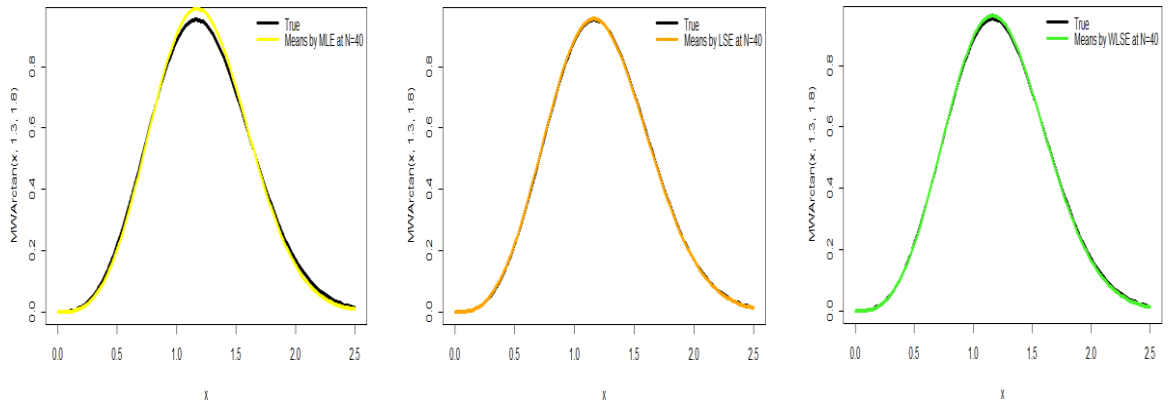

$N = 40$

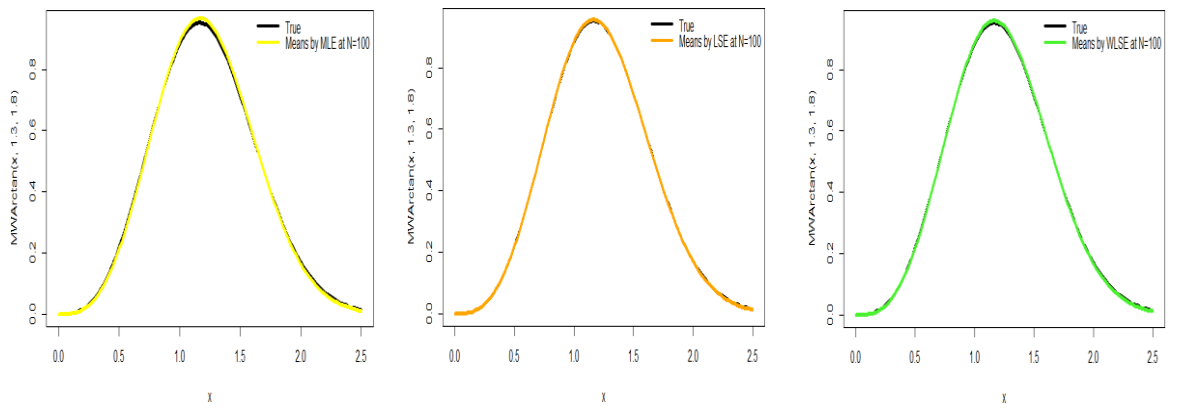

$N = 100$

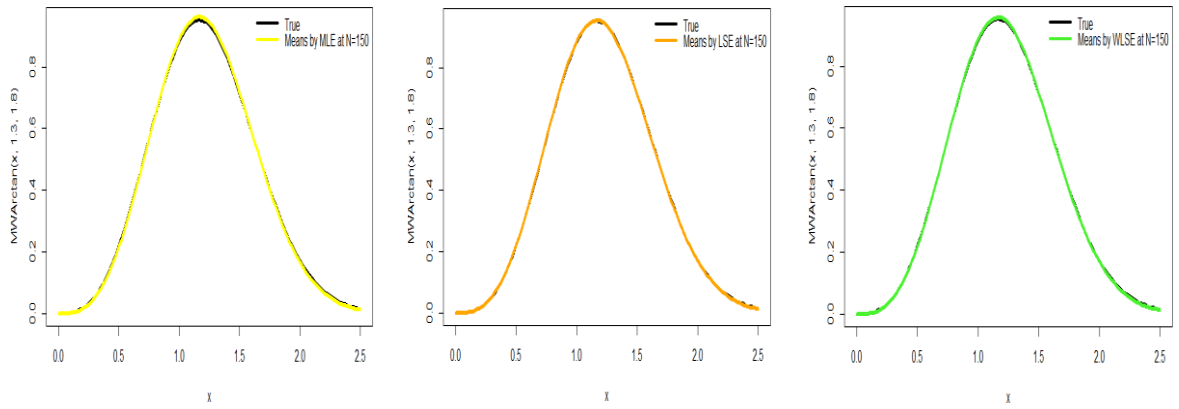

$N = 150$

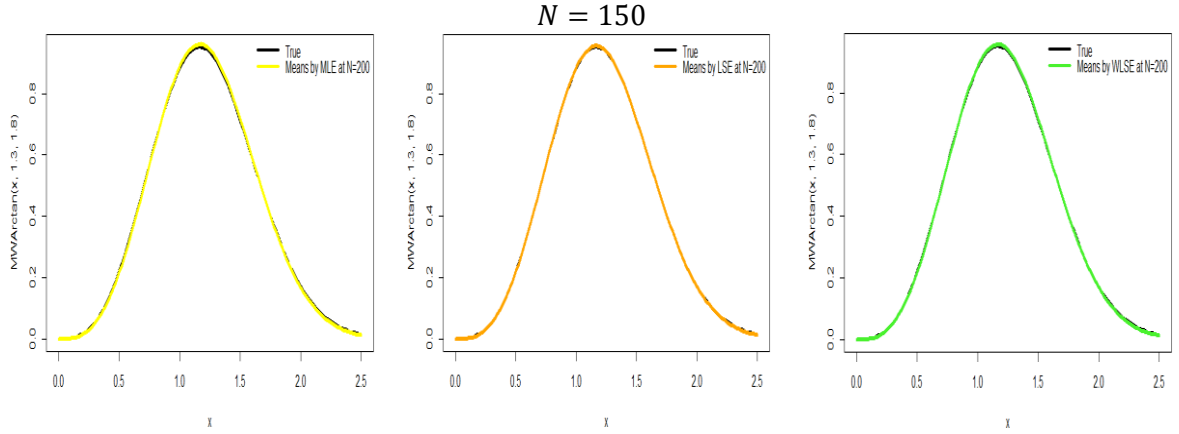

$N = 200$

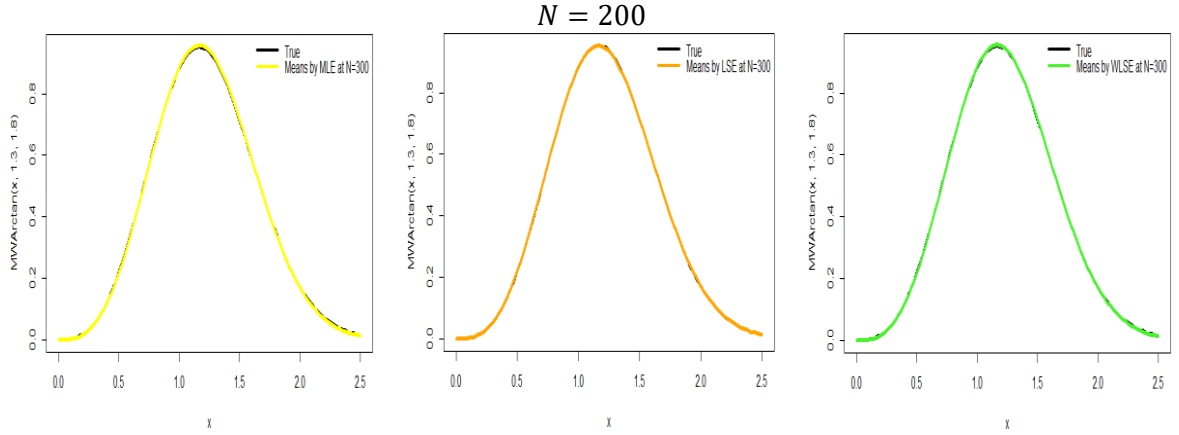

$N = 300$

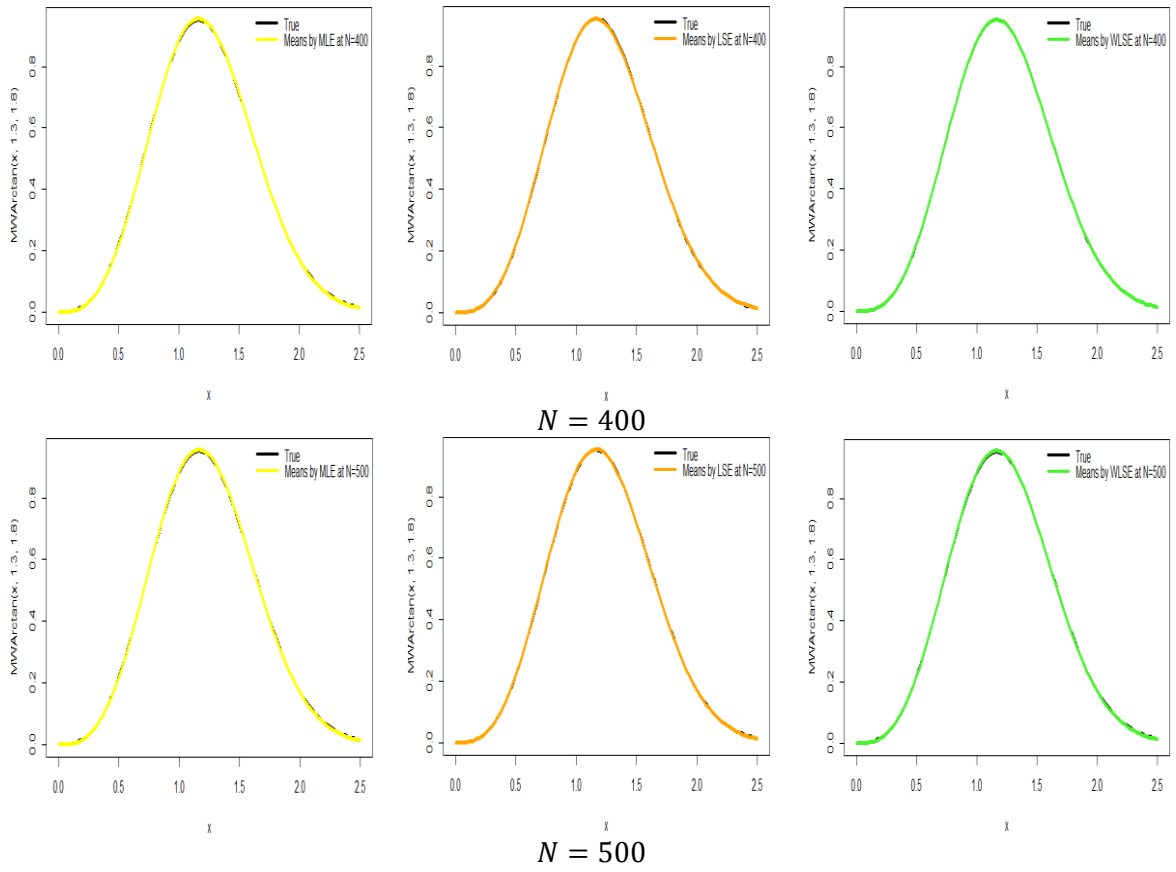

Figure 13. Comparison between pdf's for the true values and the estimated values in three methods for the sample sizes of the simulation table, case 2

To test the robustness and reliability of the results, the simulation was repeated with a different set of true parameter values. As shown in Table 3 and Figures 9–13, the performance patterns remained remarkably consistent. The results again confirmed the consistency of all estimators. The MLE estimator continued to outperform in terms of achieving the lowest MSE and RMSE values for most sample sizes, followed by the WLSE method and then the LSE method, consistent with the trends evident in Figures 10 and 11. The bias also remained low and decreasing for all methods Figure 12. The pdf comparisons in Figure 13 again demonstrate the superior performance of MLE in accurately reproducing the true shape of the distribution, especially as the sample size increases.

6. Real Data Application

The MWArctan model was applied and compared with six other competitive distributions (odd lomax Arctan (LoArctan), Kumaraswamy Arctan (KuArctan), Exponeted Generalized Arctan (EGArctan), log-gamma Arctan (LGamArctan), beta Arctan (BeArctan), and Arctan) on a real dataset representing the time-to-failure of 40 turbochargers in diesel engines are [36]: 1.6, 2.0, 2.6, 3.0, 3.5, 3.9, 4.5, 4.6, 4.8, 5.0, 5.1, 5.3, 5.4, 5.6, 5.8, 6.0, 6.0, 6.1, 6.3, 6.5, 6.5, 6.7, 7.0, 7.1, 7.3, 7.3, 7.3, 7.7, 7.7, 7.8, 7.9, 8.0, 8.1, 8.3, 8.4, 8.4, 8.5, 8.7, 8.8, 9.0.

The comparison was made using four informative criteria (AIC, CAIC, BIC, HQIC) [37], [38], [39] and four Goodness-of-fit (p-value [37], Anderson-Darling (A) [40], Cramér-von Mises (W) [41], and Kolmogorov-Smirnov (KS) [42]).

Table 4. Results of the criteria for the comparative distributions

Dist.	-L	AIC	CAIC	BIC	HQIC
MWArctan	84.12042	172.2408	172.5652	175.6186	173.4621
LoArctan	135.0518	274.1036	274.4279	277.4814	275.3249
KuArctan	91.52178	187.0436	187.3679	190.4213	188.2648
EGArctan	100.7537	205.5073	205.8317	208.8851	206.7286
LGamArctan	94.32904	192.6581	192.9824	196.0358	193.8794
BeArctan	95.92515	195.8503	196.1746	199.2281	197.0716
Arctan	101.908	207.8458	208.1702	211.2236	209.0671

Table 4 recorded the lowest value for all information criteria (AIC = 172.24, CAIC = 172.57, BIC = 175.62, HQIC = 173.46), as well as the highest value for the log-likelihood function (lowest value for -L = 84.12). This clear and tangible superiority strongly suggests that the MWArctan model is the best fit for the data among the models tested.

Table 5. Results of the criteria for the comparative distributions

Dist.	W	A	K-S	p-value
MWArctan	0.1198868	0.8503597	0.1196102	0.6162672
LoArctan	0.4572922	2.726131	0.4231447	1.202664e-06
KuArctan	0.3085412	1.939498	0.1556468	0.2871291
EGArctan	0.5765897	3.329947	0.2382167	0.02135155
LGamArctan	11.64284	76.82116	0.9997472	0
BeArctan	0.4560018	2.719419	0.1784435	0.1565
Arctan	0.5177987	3.034651	0.2635789	0.007713675

From Table 5, the MWArctan distribution stands out once again for its performance. It recorded the lowest value for the K-S statistic (0.1196) and the highest associated p-value (0.6163), meaning that the null hypothesis that the data come from the MWArctan distribution cannot be rejected at a common significance level (such as 0.05). It also recorded the lowest values for the W and A statistic (0.1199 and 0.8504, respectively). This independently confirms the results of the information criteria that MWArctan is the best fit for the data.

Table 6. Parameter estimation by MLE for comparative distributions

Dist.	$\widehat{\delta}$	$\widehat{\beta}$
MWArctan	0.002866605	2.689408451
LoArctan	178.64359	90.02732
KuArctan	26.15678	13.44256
EGArctan	2.015609	57.009340
LGamArctan	26.97153	12.07817
BeArctan	36.117102	4.826003
Arctan	1.76021	14.78509

In Table 6, the parameters were estimated using the MLE. The estimated values for the MWArctan parameters are $\delta \approx 0.00287$ and $\beta \approx 2.68941$. These values are unique to this distribution and this data and are not directly comparable to values for other distributions.

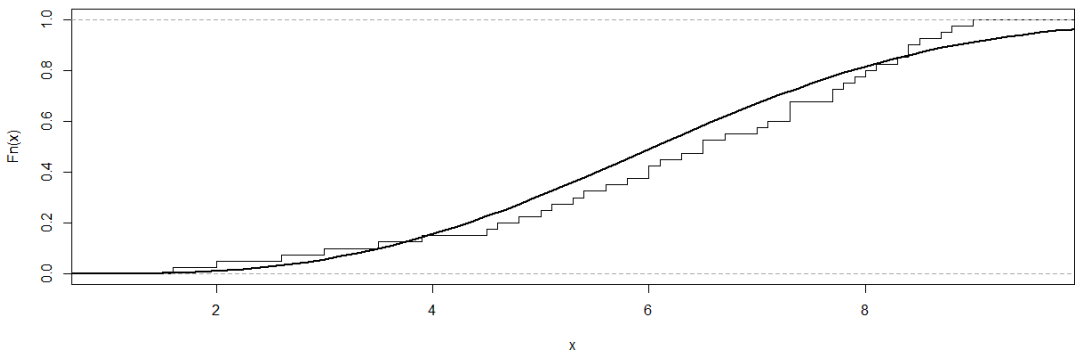

MWArctan

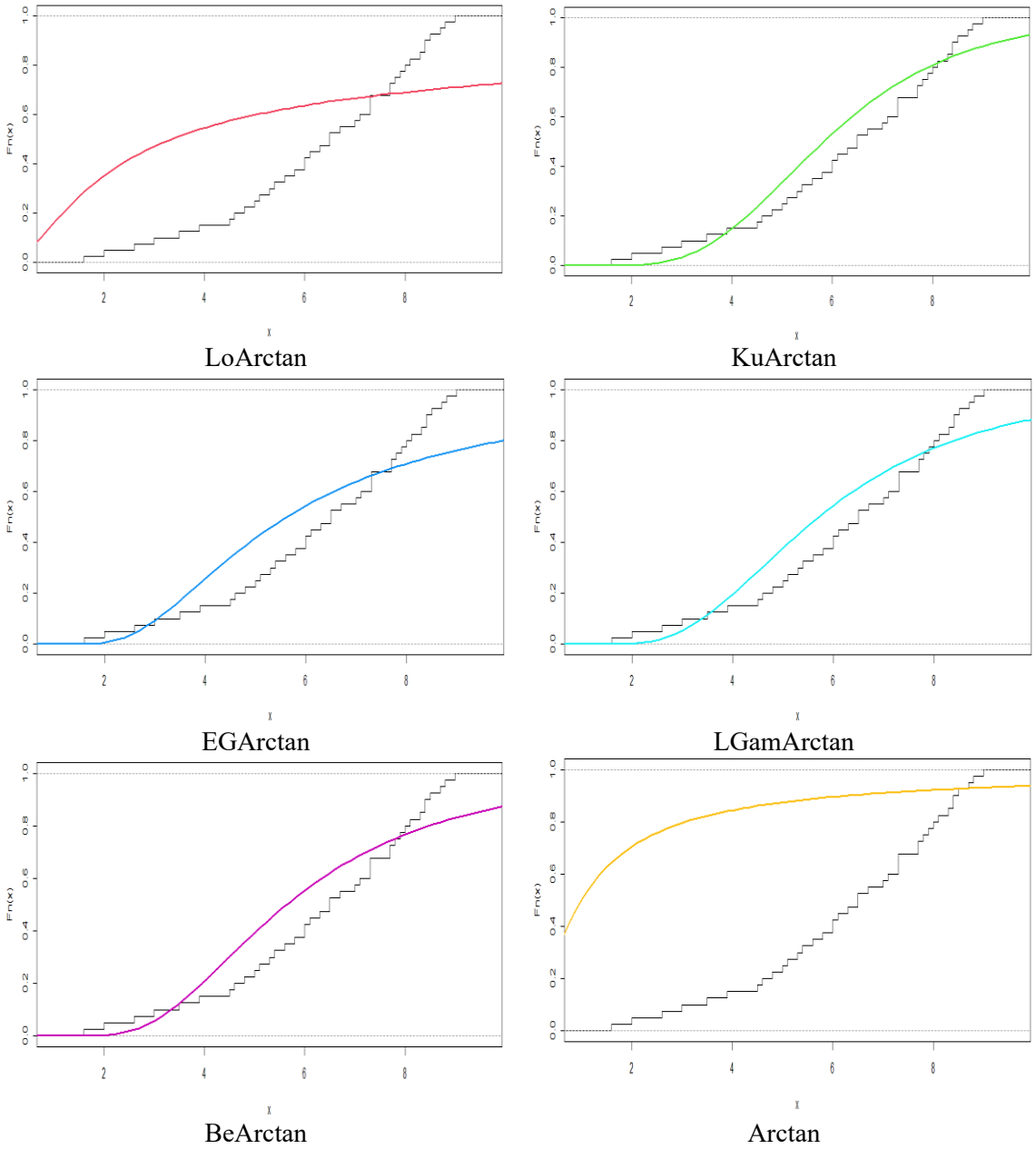

Figure 14. Empirical CDF for data set

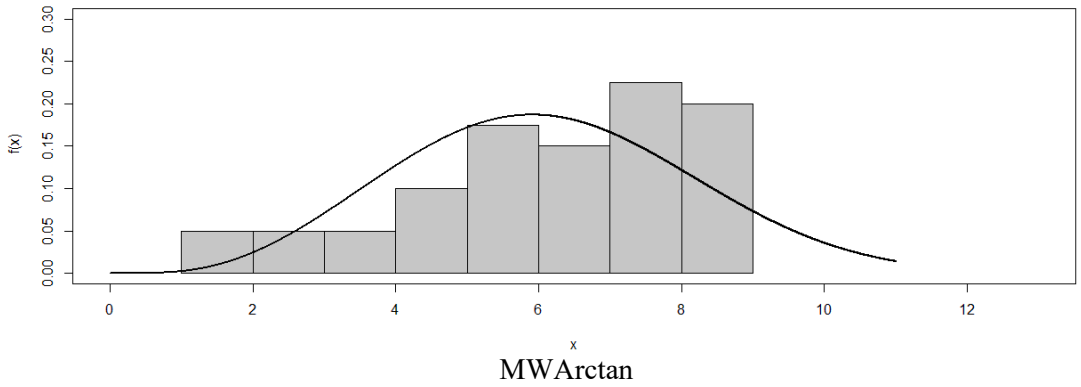

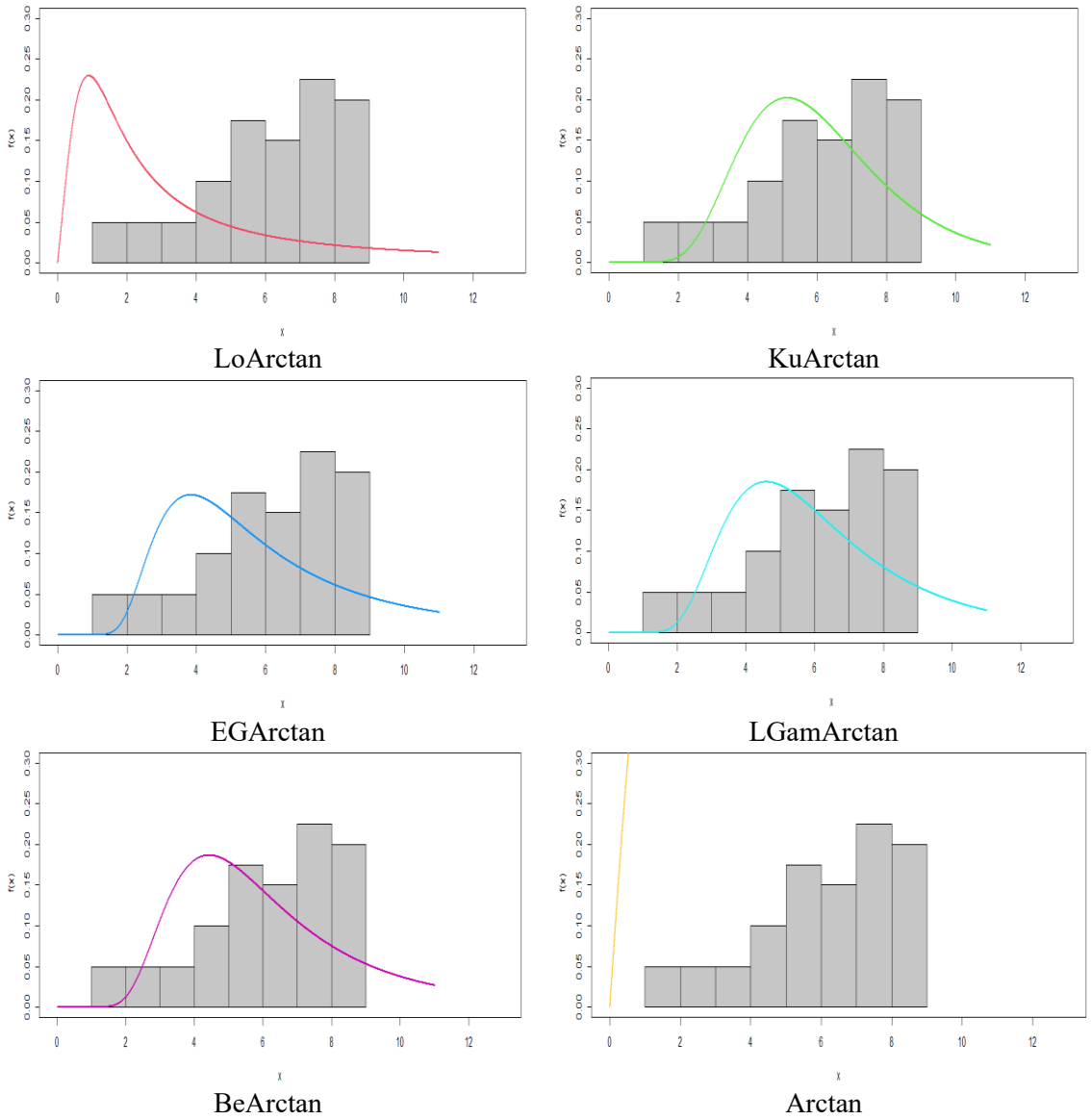

Figure 15. fitting densities for data set

Figure 14 shows how the CDF curve for the MWArctan distribution (top left) almost perfectly matches the experimental data points (bar plot). Compared to the curves of other distributions, the MWArctan fit is visually the best. Figure 15 shows the estimated density curves for the distributions over the data histogram. It is clear that the density curve for MWArctan (top left) better captures the shape of the data histogram, especially in the tails and center of the distribution, compared to other distributions that either do not fit as well as LGamArctan or fit less accurately.

7. Conclusion

The study introduced a new distribution within the MWG family using the Arctan function as a basis. This distribution has proven its high flexibility through the formulas of its basic functions and its ability to represent heavy-tailed data or data with properties that cannot be accurately represented using classical distributions. Series expansions also demonstrated the possibility of simplifying calculations related to moments and statistical properties, enhancing its usability in theoretical analysis. Furthermore, the quantile function and its derived measures (skewness and flatness) highlighted the flexibility of the distribution in handling different data types in terms of shape and dispersion. Through Monte Carlo simulations, three parameter estimation methods were compared. The results showed that MLE was the most efficient and stable method, achieving the lowest values for MSE and RMSE measures as the sample size grew, while WLSE came in second. LSE had less bias in some small samples but was associated with high variance. Practical application confirmed the superiority of MWArctan over six competing distributions, as it achieved the lowest values for information criteria and the best results in the goodness of fit tests. The graphic curves showed that MWArctan provided the closest fit to the real data, whether in the CDF or the pdf, compared to the rest of the models.

Authors' Contributions:
All authors have worked equally to write and review the manuscript.

Data Availability Statement:
The data that supports the findings of this study are available within the article.

Conflicts of Interest:
The authors declare no conflict of interest.

Funding:
This research received no external funding.

References

[1] A. S. Hassan, A. I. Al-Omari, R. R. Hassan and G. A. Alomani , "The odd inverted Topp Leone–H family of distributions: Estimation and applications," *Journal of Radiation Research and Applied Sciences,* pp. 365-379, 3 15 2022.

[2] J. T. Eghwerido, F. I. Agu and O. J. Ibidoja, "The shifted exponential-G family of distributions: Properties and applications," *Journal of Statistics and Management Systems,* pp. 43-75, 1 25 2022.

[3] Y. Wang, Z. Feng and A. Zahra, "A new logarithmic family of distributions: Properties and applications," *CMC-Comput. Mater. Contin,* p. 919–929, 66 2021.

[4] Z. Shah, D. M. Khan, Z. Khan, N. Faiz, S. Hussain, A. Anwar, T. Ahmad and K.-I. Kim, "A new generalized logarithmic–X family of distributions with biomedical data analysis," *Applied Sciences,* p. 3668, 6 13 2023.

[5] S. Hussain, M. U. Hassan, M. S. Rashid and R. Ahmed, "Families of Extended Exponentiated Generalized Distributions and Applications of Medical Data Using Burr III Extended Exponentiated Weibull Distribution," *Mathematics,* p. 3090, 14 11 2023.

[6] N. A. Noori, A. A. Khalaf and M. A. Khaleel, "A New Generalized Family of Odd Lomax-G Distributions Properties and Applications," *Advances in the Theory of Nonlinear Analysis and Its Application,* pp. 1-16, 4 7 2023.

[7] A. I. Ishaq, U. Panitanarak, A. A. Alfred , A. A. Suleiman and H. Daud, "The Generalized Odd Maxwell-Kumaraswamy Distribution: Its Properties and Applications," *Contemporary Mathematics,* pp. 711-742, 2024.

[8] G. A. Mahdi, M. A. Khaleel, A. M. Gemeay, M. Nagy , A. H. Mansi, M. M. Hossain and E. Hussam, "A new hybrid odd exponential-Φ family: Properties and applications," *AIP Advances,* 4 14 2024.

[9] N. Salahuddin, Alamgir, M. Azeem, S. Hussain and M. Ijaz, "A novel flexible TX family for generating new distributions with applications to lifetime data," *Heliyon ,* p. e36593, 17 10 2024.

[10] R. A. Abed, M. A. Khaleel and N. A. Noori, "Modified Weibull-Fréchet Distribution Properties with Application," *Iraqi Statisticians journal,* pp. 195-216, 1 2 2025.

[11] K. N. Abdullah and M. A. Khaleel, "A New Extending Inverse Weibull Distribution to Handle Neutrosophic Logic: Mathematical Properties, Parameters Estimation, and Simulation with Application," *Passer Journal of Basic and Applied Sciences,* pp. 765-782, 2 7 2025.

[12] A. Sanusi, S. Doguwa, I. Audu and Y. M. Baraya, "Topp Leone Exponential – G Family of Distributions: Properties and Application," *NIPES Journal of Science and Technology Research,* pp. 83 -96, 4 2 2020.

[13] A. A. Al-Babtain, M. K. Shakhatreh, M. Nassar and A. Z. Afify, "A new modified Kies family: Properties, estimation under complete and type-II censored samples," *Mathematics and engineering applications,* p. 1345, 8 8 2020.

[14] N. A. Noori, A. A. Khalaf and M. A. Khaleel, "A new expansion of the Inverse Weibull Distribution: Properties with Applications," *Iraqi Statistians Journal,* pp. 52-62, 1 1 2024.

[15] A. M. Almarashi, J. Farrukh , C. Chesneau and M. Elgarhy, "A new truncated muth generated family of distributions with applications," *Complexity ,* p. 1211526, 1 2021.

[16] A. Z. Afify, H. Al-Mofleh, H. M. Aljohani and G. M. Cordeiro, "The Marshall–Olkin–Weibull-H family: Estimation, simulations, and applications to COVID-19 data," *Journal of King Saud University – Science,* p. 102115, 34 2022.

[17] N. A. Noori and M. A. khaleel, "Estimation and Some Statistical Properties of the hybrid Weibull Inverse Burr Type X Distribution with Application to Cancer Patient Data," *Iraqi Statisticians Journal,* pp. 8-29, 2 1 2024.

[18] A. Khaoula, N. Seddik-Ameur, A. A. Abd El-Baset and M. A. Khaleel, "The Topp-Leone Extended Exponential Distribution: Estimation Methods and Applications," *Pakistan Journal of Statistics and Operation Research,* pp. 817-836, 4 18 2022.

[19] A. M. Abd El-latif, O. A. Alqasem, J. K. Okutu, C. Tanış, L. P. Sapkota and N. A. Noori, "A flexible extension of the unit upper truncated Weibull distribution: Statistical analysis with applications on geology, engineering, and radiation Data," *Journal of Radiation Research and Applied Sciences,* p. 101434, 2 18 2025.

[20] N. A. Noori, M. A. Khaleel, S. A. Khalaf and S. Dutta, "Analytical Modeling of Expansion for Odd Lomax Generalized Exponential Distribution in Framework of Neutrosophic Logic: a Theoretical and Applied on Neutrosophic Data," *Innovation in Statistics and Probability,* p. 47–59, 1 1 2025.

[21] F. A. Bhatti, G. G. Hamedani, M. C. Korkmaz, G. M. Cordeiro, H. M. Yousof and M. Ahmad , "On Burr III Marshal Olkin family: development, properties, characterizations and applications," *Journal of Statistical Distributions and Applications,* pp. 1-21, 6 2019.

[22] G. O. Orji, H. O. Etaga, E. M. Almetwally, C. P. Igbokwe, O. C. Aguwa and O. J. Obulezi, "A New Odd Reparameterized Exponential Transformed-X Family of Distributions with Applications to Public Health Data," *Innovation in Statistics and Probability,* pp. 88-118, 1 1 2025.

[23] I. A. Sadiq, S. I. S. Doguwa, A. Yahaya and J. Garba, "NEW GENERALIZED ODD FRÉCHET-ODD EXPONENTIAL-G FAMILY OF DISTRIBUTION WITH STATISTICAL PROPERTIES AND APPLICATIONS," *FUDMA Journal of Sciences (FJS),* pp. 41 - 51, 6 7 2023.

[24] N. Eugene, L. Carl and F. Famoye, "Beta-normal distribution and its applications.," *Communications in Statistics-Theory and methods,* pp. 497-512, 4 31 2002.

[25] G. P. Dhungana and V. Kumar, "Exponentiated Odd Lomax Exponential distribution with application to COVID-19 death cases of Nepal," *PloS one,* p. e0269450, 6 17 2022.

[26] H. J. Gómez, K. I. Santoro, I. B. Chamorro, O. Venegas, D. I. Gallardo and H. W. Gómez, "A Family of Truncated Positive Distributions," *Mathematics,* p. 4431, 21 11 2023.

[27] M. Y. Mustafa and Z. Y. Algamal, "Neutrosophic inverse power Lindley distribution: A modeling and application for bladder cancer patients," *International Journal of Neutrosophic Science,* pp. 216-223, 2 21 2023.

[28] A. R. El-Saeed, N. A. Noori, M. A. Khaleel and S. M. Alghamdi, "Statistical properties of the Odd Lomax Burr Type X distribution with applications to failure rate and radiation data," *Journal of Radiation Research and Applied Sciences,* p. 101421, 2 18 2025.

[29] A. N. Nooruldeen, A. k. Mundher and D. A. Dalya , "The Modified Burr-III Distribution Properties, Estimation, Simulation, with Application on Real Data," *Iraqi Statisticians Journal,* pp. 225-246, special issue for ICSA2025 2 2025.

[30] K. H. Al-Habib, M. A. Khaleel and H. Al-Mofleh, "A new family of truncated nadarajah-haghighi-g properties with real data applications," *Tikrit Journal of Administrative and Economic Sciences,* p. 2, 61 19 2023.

[31] N. A. Noori, "Exploring the Properties, Simulation, and Applications of the Odd Burr XII Gompertz Distribution," *Advances in the Theory of Nonlinear Analysis and Its Application,* pp. 60-75, 4 7 2023.

[32] M. Q. Ibrahim, A. A. Mohammed, A. A. Khalaf and N. A. Noori, "Comparative Analysis of Seasonal Mixed Integrated Autoregressive Moving Average and Feed-Forward Neural Networks Models in Predicting United State Natural Hazard Casualties," *Baghdad Science Journal,* pp. 2360-2374, 7 Article 22 22 2025.

[33] A. A. Khalaf, M. Q. Ibrahim and N. A. Noori, "[0,1]Truncated Exponentiated Exponential Burr type X Distributionwith Applications," *Iraqi Journal of Science,* pp. 4428-4440, 8 65 2024.

[34] . M. Albassam, N. Khan and M. Aslam, "The W/S test for data having neutrosophic numbers: An application to USA village population," *Complexity,* pp. 1-8, 2020.

[35] D. D. Ahmed and M. A. Khaleel, "The Gompertz Nadarajah-Haghighi (GoNH) Distribution Properties with Application to Real Data," *Iraqi Journal for Computer Science and Mathematics,* p. 11, 3 5 2024.

[36] K. Xu, M. Xie, L. C. Tang and S. L. Ho, "Application of neural networks in forecasting engine systems reliability," *Applied Soft Computing,* pp. 255-268, 4 2 2003.

[37] K. N. Abdullah, N. A. Noori and M. A. khaleel, "Data Modelling and Analysis Using Odd Lomax Generalized Exponential Distribution: an Empirical Study and Simulation," *Iraqi Statisticians Journal,* pp. 146-162, 1 2 2025.

[38] N. A. Noori, D. D. Ahmed and M. A. Khaleel, "Odd Lomax Chen distribution: An Innovative Statistical Tool for Improving Real Data Modeling and Its Practical Applications," *Tikrit Journal of Administrative and Economic Sciences,* pp. 1098-1126, Special Issue, Part (1) 21 2025.

[39] N. A. Noori, K. N. Abdullah and M. A. Khaleel, "Data Modelling and Analysis Using Odd Lomax Generalized Exponential Distribution: an Empirical Study and Simulation," *Iraqi Statisticians journal,* pp. 146-162, 1 2 2025.

[40] M. M. Rahman, A. M. Gemeay, M. A. I. Khan, M. A. Meraou, M. E. Bakr, A. H. Muse, E. Hussam and O. S. Balogun, "A new modified cubic transmuted-G family of distributions: Properties and different methods of estimation with applications to real-life data," *AIP Advances,* p. 095025, 9 13 2023.

[41] M. Aslam, Z. Asghar, Z. Hussain and S. F. Shahc, "A modified TX family of distributions: classical and Bayesian analysis," *Journal of Taibah University for Science,* pp. 254-264, 1 14 2020.

[42] S. Naz, L. A. Al-Essa, H. S. Bakouch and C. Chesneau, "A transmuted modified power-generated family of distributions with practice on submodels in insurance and reliability," *Symmetry ,* p. 1458, 7 15 2023.